University of Tartu
Faculty of Science and Technology
Institute of Ecology and Earth Sciences
Department of Geography

Master Thesis in Geoinformatics for Urbanized Society (30 ECTS)

Urban Sprawl Dynamics and Urban Heat Islands (UHI) in Ghana

Isaac Newton Kwasi Buo

Supervisors: Valentina Sagris PhD
Iuliia Burdun MSc

Approved for defense:
Supervisor:
Head of Department:

Tartu 2019

Magistritöö linnastunud ühiskonna geoinformaatikas: alglinnastumise dünaamika ja linna soojussaared (UHI) Ghanas

Kokkuvõte

Linnalised alad puutuvad kasvades kokku kahe nähtusega. Esimene neist on valglinnastumine, mida iseloomustab linnade laienemine väljapoole. Teine nähtus on linna soojussaared (UHI), mida põhjustavad peamiselt vett mitteläbilaskvad ja kuumust koguvad materjalid, millega linnastumise käigus asendatakse looduslik maapind. Neil nähtustel on mõju linnaruumi õhukvaliteedile, linnaelanike tervisele ja ka majanduslik mõju linnaelanikele ja valitsusele.

Valglinnastumise kohta on olemas mitmeid uuringuid ning kirjanduses pakutakse välja viise selle tuvastamiseks ja mõõtmiseks. Troopiliste alade UHI-d on kõige vähe uuritud, kuigi selle piirkonna linnastumise määr on globaalses mastaabis kõige kiirem. Satelliitkaugseire andmed võimaldavad koostada maakatte kaardid, kasutades klassifitseerimist, et tuvastada valglinnastumise alad. Termiline kaugseire annab andmed maapinna temperatuuri (LST) hindamiseks. LST on aluseks UHI-de analüüsile. UHI-de hindamine LST kaudu annab tulemuseks maapinna soojussaare (SUHI).

Uuringus keskenduti valglinnastumise iseloomustamisele kahes Ghana linnas (Accra ja Kumasi) 15-aastase perioodi vältel (2002–2017). Samuti teostati kahe linna valglinnastumise võrdlusanalüüs ning analüüsiti valglinnastumise mõju SUHI-le. Analüüsiks kasutati kaugseire andmeid. Tulemused näitavad linnaliste alade laienemise olemust mõlemas linnas ja uuringuperioodil domineerivaid linnalisi protsesse. Samuti sisaldavad tulemused andmeid UHI intensiivsuste ja kuumade alade kohta uuringupiirkondades.

Märksõnad: valglinnastumine, linna soojussaar, kaugseire, maapinna kate, maapinna temperatuur.

CERCS kood: T181 Kaugseire

Master Thesis in Geoinformatics for Urbanized Society: Urban Sprawl Dynamics and Urban Heat Islands (UHI) in Ghana

Abstract

Urban areas face two potential phenomena as they burgeon. The first is the urban sprawl characterized by outward expansion of urban areas. The second is Urban Heat Islands (UHI), which is primarily caused by impervious and heat-trapping materials replacing the natural land cover during urbanization. These phenomena have impacts on the air quality and health of urban dwellers and economic impacts on citizens and government.

Numerous studies exist on urban sprawl and several means of detecting and measuring it are suggested in the literature. UHI in the tropical climates is the least studied even though urbanization rate in the region is the fastest on a global scale. Data from sensors aboard Earth-orbiting satellites allows for the generation of land cover maps through image classification to detect sprawl. Thermal remote sensing imagery provides the relevant data for estimating Land Surface Temperature (LST), on which the UHI analysis is made. Assessing UHI with LST qualifies it as Surface Urban Heat Islands (SUHI).

This research focused on sprawl in two tropical Ghanaian cities namely Accra and Kumasi over a 15-year period (2002-2017). Sprawl in both cities was compared and its influence on SUHI was analyzed. Remotely sensed satellite imageries were employed for the analysis. The results reveal the nature of urban expansion in both cities and the dominant urban processes for the study period. Also, the UHI intensities and the hot regions within the study areas are captured in the results.

Keywords: Urban sprawl, Urban Heat Island, Remote Sensing, Land Cover, Land Surface Temperature.

CERCS Code: T181 Remote sensing

Contents

Introduction

As the human population increases, demand for housing and other necessary infrastructure to make life comfortable becomes high. Consequently, rural areas become urbanized to meet the growing demand (Bharath et al., 2018). Whereas this is a widely accepted form of urbanization, what may be classified as rural or urban is subjective (McGranahan and Satterthwaite,2014). According to McGranahan and Satterthwaite (2014), the United Nations assessment on rural and urban populations is based on variants of definitions of both terms from different countries. They further report that these definitions are based on criteria such as population sizes and densities. For instance, in Sweden, a built-up area of 200 households with 200 meters or less spacing between them will qualify as urban whereas 40,000 inhabitants must live in an area to make it urban in Mali (McGranahan and Satterthwaite,2014).

As rural areas gradually become urban there is a tendency of urban sprawl phenomenon occurring, which is characterized by outward expansion of an urban area towards its boundaries in an unplanned and uncontrolled manner (Karakayaci, 2016; Antrop 2018). Furthermore, another identified direct consequence of the transformation of rural spaces to urban ones is the replacement of natural land with impervious and heat-trapping surfaces such as concrete and asphalt (Madanian et al., 2018). Aside the alteration of the natural landscape by this act of land cover replacement, the exchange of energy between the land surface and the atmosphere is altered thereby affecting microclimatic variables such as temperature and winds near the surface (Madanian et al., 2018). The effect on microclimatic variables such as temperature results in the phenomenon termed as Urban Heat Islands (UHI) (Voogt and Oke, 2002). In this research, portions within the study area with low built-up densities are classified as rural and those with high densities as urban.

UHI has an impact on the health of humans as it has been noted to facilitate the decline in air quality and impaired water quality (US-EPA, 2008). Santamouris et al. (2005), note that the impact of the phenomenon is not only limited to health but includes economic impacts as well. The health impacts of the phenomena have been experienced globally, primarily through heat waves which are facilitated by UHI (US-EPA, 2008). In tropical regions the WMO and WHO (2015) state that heat waves which hitherto were no threats are now a concern due to urbanization and its accompanying UHI. Codjoe and Nabie (2014) established a positive relationship between Cerebrospinal Meningitis incidence and warm temperatures in Ghana. WMO and WHO (2015) also identified that high temperatures promoted breading of disease spreading pathogens. As established by Nabi and Qader (2009), malaria, a killer in the tropics is prevalent in such areas because the climate and temperature are suitable for mosquitoes and the Plasmodium parasites. Hence if the warming increases because of UHI in these areas then the eradication of malaria will be prolonged.

Although UHI occurrence may not be discriminatory as it only occurs in areas where anthropogenic activities and developments facilitate it, there are levels of vulnerabilities when it comes to its impacts (Filho et al. 2018, Sagris and Sepp, 2016, van der Hoeven and Wandl, 2018). The vulnerabilities levels among citizens may result from differences in age (Sagris and Sepp, 2016, van der Hoeven and Wandl, 2018) or financial capabilities (Thomas and Butters, 2017). These differences among citizens tend to have an influence on where they choose to live within an urban space which results in segregation (van Ham et al., 2016). Segregation introduces a spatial dimension to the vulnerability levels of UHI impact as some people may suffer more giving where they live, or work compared to others (Thomas and Butters, 2017).

Whether health or economic impact on citizens or government, an undeniable impact of UHI on an urban area is how it undermines the liveability of the place (Sidiqui et. al, 2016). Air quality and health are key dimensions of liveable places (Kennedy and Buys, 2010). Therefore, a negative impact on these dimensions by a phenomenon in any area warrants research into the characterization of the phenomenon to suggest bespoke mitigation measures (Sidiqui et. al, 2016).

Many studies have been made to investigate sprawl or expansion and how it relates to UHI. Most researchers delineate urban areas using supervised classifications algorithms in both pixel-based and object-based approaches (Li et al., 2018; Li et al., 2009; Silva et al., 2018; Wei and Blaschke, 2018). Al-doski et al (2013) described the process as one where software is trained to classify pixels based on sites identified by the analyst to represent a class. A few researchers have achieved this by employing spectral indices with examples in Xu et al (2009) and Kimuku and Ngigi (2017). In these researches, derived land surface temperatures are combined with land cover/land use using GIS techniques to identify heat islands. Computing a heat island intensity is a shortfall of most sprawl and UHI combined research as the interest is primarily about delineating the heat islands or showing its footprints.

The research focused on identifying sprawls and their extent in two major Ghanaian cities (Accra and Kumasi) over the period of 2002 to 2017 using remote sensing imagery, identifying UHI in the cities and ultimately finding out how sprawl influenced the UHI in these cities over the study period. Hence, the research sought to answer the following questions;

1. What is the extent of urban sprawl in the two Ghanaian cities in the period 2002 to 2017 and how they both compare?

2. How Urban sprawl affected UHI extent and magnitude in the study areas?

This report has five chapters. The first provides a theoretical overview of the phenomena under investigation and an overview of sprawl and climate conditions in the study area. The second chapter covers the data collected and the methods used. The third chapter focuses on the results of the analysis done. The fourth chapter is a discussion of the methods and the results of the research. Finally, the last chapter provides conclusions to this research.

1. Theory

1.1 Definition of urban sprawl, causes, and effects

Urban sprawl is a phenomenon that is complex to define. Bhatta et al. (2010) and Wilson et al. (2003) suggest that it is worth describing the phenomenon than defining it. Whereas Galster et al. (2001) are of the opinion the terminology is one name for many conditions which explains everything and nothing. Irrespective of the admission of the fact that urban sprawl is hard to define, attempts have been made to define it. It is worth noting that these definitions are usually limited to the scope of the research. Galster et al. (2001) defined it as a condition of land use that is represented by low values on one or more of eight dimensions (density, continuity, concentration, clustering, centrality, nuclearity, mixed uses, and proximity) of land use patterns in their research. Ewing (2008) suggests that sprawl is broadly definable as 'undesirable' scattered development, leapfrog development, strip or ribbon development, or continuous low-density development. Another perspective defines urban sprawl as a transition zone with indefinite borders between rural and urban areas (Karakayaci, 2010). Antrop (2018), also defines it as an uncoordinated expansion of human habitat away from urban centers into low-density, mono-functional and usually car-dependent communities, and no holistic planning view. Bhatta et al. (2010) identified that existing literature suggested that "sprawl can alternatively or simultaneously refer to (1) certain patterns of land-use, (2) processes of land development, (3) causes of particular land-use behavior, and (4) consequences of land-use behaviors". Irrespective of the varying definitions, the consensus is that urban sprawl is characterized by an unplanned and uneven pattern of growth, driven by a multitude of processes and leading to inefficient resource utilization (Bhatta, 2010).

The sprawl phenomenon is driven primarily by two factors which are population growth and migration from rural to urban areas (Karakayaci, 2010; Bhat et.al, 2017). Sprawling is noted to result in injudicious use of space and the destruction and change of the natural landscape (Karakayaci, 2016; Antrop, 2018). One notable change in land use is the loss of agricultural land which has an economic impact on society and hinders regional sustainable development (Karakayaci, 2016; Bhat et.al, 2017). Sprawl creates car-dependent neighborhoods which are known to have an impact on air quality given the emission of carbon, and obesity among the populace due to poor physical activity (Karakayaci, 2016; Frumkin, 2002; Freudenberg et al., 2005). These impacts are of major concern to policymakers and motivation for researchers to develop metrics for characterizing and measuring sprawl.

1.1.1 Measurement of sprawl

There are many methods for measuring the phenomenon just as there are many definitions of it. First, the measurement of sprawl according to Bhatta et al. (2010) may be on an absolute or a relative scale. Absolute in this context provides a distinction between a sprawled urban space and one which is not. Relative measures, in contrast, quantify several attributes of urban growth that can be compared among cities, among different zones within a city, or among different times(periods) for a city (Bhatta, 2010, Orenstein and Frenkel, 2012).

Defining a threshold by which an urban space can be classified as sprawled has been difficult to realize (Bhatta, 2010). Therefore, a good deal of metrics has been employed by different researchers to quantify the phenomenon (on relative scales). Galster et al. (2001) identified *density, continuity, concentration, clustering, centrality, nuclearity, mixed uses, and proximity* as eight basic dimensions by which sprawl can be quantified. They assert that these dimensions are conceptual, objective and measurable for every urban land use and a low value of any of them or a combination of some will indicate sprawl. Angel et al. (2007) proposed five metrics for measuring sprawl: which are the *main urban core, secondary urban core, urban fringe, ribbon development and scatter development*. These metrics are further defined by conditions set by researchers. Angel et al. (2007) classified built-up

pixels into these proposed metrics based on their relationship with neighboring pixels. It further suggests that these metrics can be reused in cases with user-defined rules.

Advancement in GIS and remote sensing technologies has provided the opportunity to combine GIS analysis with descriptive statistical analysis to quantify sprawl Bhatta (2010). This owes to the fact that sprawl is a phenomenon that occurs in the domain of space and time. In addition, these technologies provide data of high spatial accuracy with an affordance of analysis for detecting, measuring and characterizing sprawl in recent researches (Bhatta, 2010; Gandhi et al., 2016). Research works done by (Jat et al., 2007; Osei et al., 2015) where Shannon's entropy was used as a metric with GIS methods to measure sprawl are quintessential cases. Bhatta (2010), further assets that Shannon's entropy approach is the most widely used. An underlying activity common to these methods is the classification of land cover which enables the usage of a metric to be used to quantify sprawl to some extent. An integral aspect of the classification of land cover is the detection of impervious surfaces (Irwin and Bockstael, 2007). Remote sensing data has been the most preferred choice for such classification (Bhatta, 2010).

1.2 Urban heat islands

Urban Heat Islands is the terminology for the phenomenon where urban areas experience higher temperature compared to their surrounding non-urban areas because of urban surfaces (Schwarz et al. 2011). Figure 1 is a pictographic representation of the phenomenon based on this definition. Voogt and Oke (2002), defined the phenomenon as surface and atmospheric modifications due to urbanization which leads to a modified thermal climate that is warmer than the surrounding non-urbanized areas, particularly at night. Li (2018) corroborates this by asserting that land use change caused by urbanization is the primary driving factor of UHI. Wong et al (2010), further assert that the complexity of constructions and anthropogenic heat discharge due to human activities also cause UHI. The change in land use can relate to the replacement of natural land cover with impervious and heat-trapping materials such as asphalt and concrete.

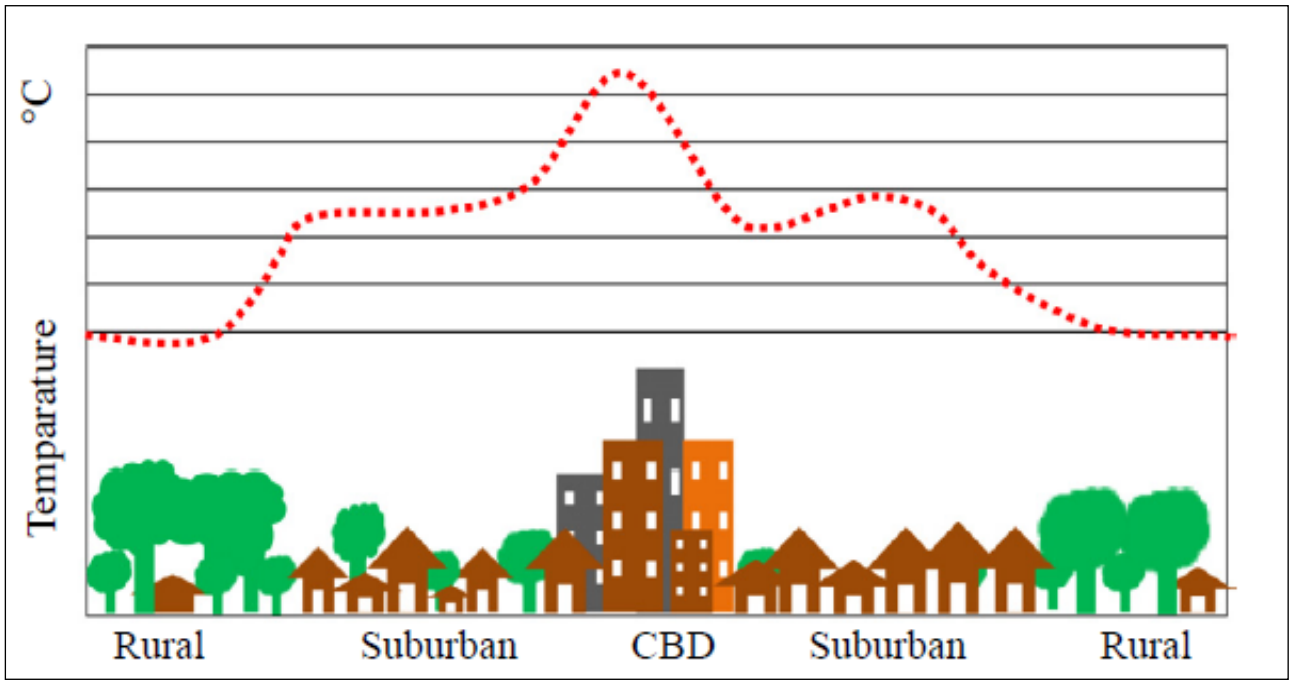

Figure 1. *Urban heat island profile (Source: Bhargava, 2017)*

UHI, depending on the way of formation, techniques used in their identification and measurements may be classified as Surface Urban Heat Islands (SUHI) or Atmospheric Urban Heat Islands (AUHI) (US-EPA, 2008). SUHI is derived from measurement of air temperature above ground usually less than 2 meters (Sagris and Sepp, 2016; Schwarz et al 2011) whereas AUHI encompasses all measurements made above 2 m (US-EPA, 2008). The US-EPA (2008) further classifies AUHI into canopy layer and boundary layer, where canopy will refer to UHI based on measurements made between 2m to 1.5km above the surface and boundary layer measurements beyond 1.5km. SUHI has been the preferred method for the appraisal of the phenomenon given the advancement of remote sensing technologies which make it possible (van der Hoeven and Wandl, 2018).

1.2.1 SUHI measurements and delineation

Measurement of SUHI has long been studied by ground-based observations taken from fixed thermometer networks (Voogt and Oke, 2002; Schwarz et al. 2011). With the advent of thermal remote sensing technology, remote observation of SUHIs became possible using sensors aboard satellites. Land Surface Temperatures (LST) which is commonly used indicator for UHI can be estimated with high accuracies with data from these sensors (Voogt and Oke, 2002; Schwarz et al 2011; Meng et al 2018). In contrast to the direct ground measurements, the remotely sensed SUHI is an indirect measurement requiring consideration of the intervening atmosphere and the surface radiative properties that influence the emission and reflection of radiation within the spectral wavelengths detected by the sensor (Voogt and Oke, 2002).

The difference in mean LST between urban areas and rural/sub-urban areas provides the intensity of SUHI which Sagris and Sepp (2016) indicate there are a plethora of algorithms available for its calculation. An issue in the measurement is the clear delineation of urban and rural boundaries. In Schwarz et al (2011), rural is defined as parts of a city region that are not influenced by the urban heat island. Other researchers have also defined rural and urban using land cover. Meng et al (2018) introduced the extraction of the Urban Built-up Area (UMBA) based on biophysical composition index and distance-weighted impervious surface distribution density. The Index-based Built-up Index (IBI) and Normal Difference Building Index (NDBI) have been also employed as measures to delineate urban areas from rural areas (Xu et al 2009; Kimuku and Ngigi, 2017). The choice of method or combination of methods is subject to the study area characteristics, data employed, and judgments of the researcher as various methods have been deemed useful in the context in which they were used. To further appreciate the phenomenon at a given place, it is good practice to analyze the delineated islands on certain scales such as variations in time or variations based on differences in spatial locations. In Meng et al. (2018), an additional statistical analysis was conducted to identify the diurnal variations in the SUHI. Elsewhere, Ward et al. (2016), reveal how the size in terms of area of heat islands had a significant influence of the Surface Urban Heat Island Magnitude in 70 European cities for a specified period. Hence SUHI can be assessed by way of spatial extent or magnitude over time.

SUHI has a wide range of effects on the health of urban dwellers. Sagris and Sepp (2016) report that over 14,000 deaths in France in 2003 were because of heat waves. In the Indian city of Allahabad, heatwave studies revealed that mortality in the month of May 2010 increased by 40% compared to the average of previous years as temperatures exceeded 45 °C (Thomas and Butters, 2017). Economically, SUHI raises the demand for energy for cooling in buildings (Santamouris et al., 2015; Akbari, 2005). Furthermore, Wong et al (2017) stress that the impact of the phenomenon on human health has a negative effect on labor productivity in urban areas. Thomas and Butters (2017) indicate that the use of Air Conditioning (AC) is a mundane remedy to the discomfort caused by UHI in tropical urban areas. They further note that this remedy is a luxury and a privilege of the rich few. This suggests that the discomfort in these areas are mostly experienced by poor people, who live in buildings with woeful thermal insulations and spend a greater part of their day outdoors (Thomas and Butters,2017; Amorim and Dubreuil, 2017). Thomas and Butters (2017) explain that the dependence AC in these urban areas

contributes to the UHI phenomenon through thermal energy emissions from the units to the immediate street environment. Therefore, a cause of the phenomenon is unending, and the repercussions are suffered the most by the less privileged. The implication is that economic differences among citizens influence their exposure to the effects of UHI.

Giridharan and Emmanuel (2018) reveal that much of the 21st century global urbanization is concentrated in the developing world and a vast swathe of this lies in the Tropical (23.5^{o} N and 23.5^{o} S) and sub-tropical zones (up to 30^{o} N and 30^{o} S), within the three 'tropical' sub-climate types as defined by the Köppen-Geiger climate classification: Tropical Rainforest or, Tropical Monsoon and Tropical Wet and Dry or Savannah. Despite the growing population in the tropics and its rapid urbanization, the nature of local climate change induced by urban growth is not well studied and by extension UHI in the region as well (Giridharan and Emmanuel, 2018; Rajagopalan et al.2014). The number of studies on UHI in temperate regions far outweighs those carried out in tropical zones according to Rajagopalan et al. (2014) although it is a global phenomenon and its warming effect is considered as a quintessential local climate change according to US-EPA (2008).

1.3 Urbanization and urban sprawl in Ghana

Ghana like other developing countries in Africa has an increasingly urban population. This results in the extension of urban areas and the conversion of vegetated lands into built-up areas. Urban space in Ghana is defined as a place (Settlement) with a population of 5,000 or more persons (Songsore, 2009). The World Bank Group (2015) reveals that the country has witnessed rapid urbanization especially in major cities in the last three decades and describes it as momentous (Figure 2). The urbanization has been attributed to the natural increase of population, migration, and restructuring of district, municipal and metropolitan boundaries (Ghana Statistical Services 2014a; Ardayfio-Schandorf et al., 2012). The population was noted to double between the period of 1984 and 2013 with urban population growing at 4.4 percent per annum (World Bank Group, 2015; Ardayfio-Schandorf et al., .2012). In addition, the growth in urban population for the period outpaced the growth in rural population. The growth since 1984 the World Bank Group (2015) attributes to the recovery of the national economy and improved urban economic opportunities. The adoption of a new constitution and switch to democratic governance since 1992, has propelled urbanization going forward. Cobbinah and Aboagye (2017), attributed the causes of sprawl in Ghana to a multiple of factors, which comprised the land tenure system and means of acquiring title to land, under-resourced and ineffective urban planning agencies in Ghana. Owusu (2013), asserts that the nation's open-door policy towards global capital and free movement of people within the West African region fuels the urbanization process.

The urbanization being experienced by Ghana's three largest urban areas (Figure 3) Accra, Kumasi, and Sekondi-Takoradi has not spared them from the phenomenon of urban sprawl. Urban sprawl patterns for Accra and Kumasi were found to be identical to each other in Stow et al. (2016). Based on land use and land cover comparison made for the years 2000 and 2010 for Kumasi and Accra, Stow et al. (2016) reported that 52% of the newly built-up areas occurred in the fringes (peri-urban and sub-urban) of both cities which are corroborated by Acheampong et al., (2016) and Abass et al. (2018) in the case of Kumasi. According to Stemn and Agyapong (2014), sprawl in Sekondi-Takoradi is characterized by outward expansion, ribbon development, and densification. Development in Accra is mainly an outward expansion from the center (Oduro et al., 2014; Osei et al 2015). Sprawl in Ghana can be in the form of neighborhood segregations (Cobbinah and Aboagye, 2017), leapfrog developments (Cobbinah and Aboagye, 2016; Owusu, 2013; Owusu-Ansah and O'Connor, 2010), patchy, dotted and outward development (Cobbinah and Aboagye, 2016; Owusu, 2013).

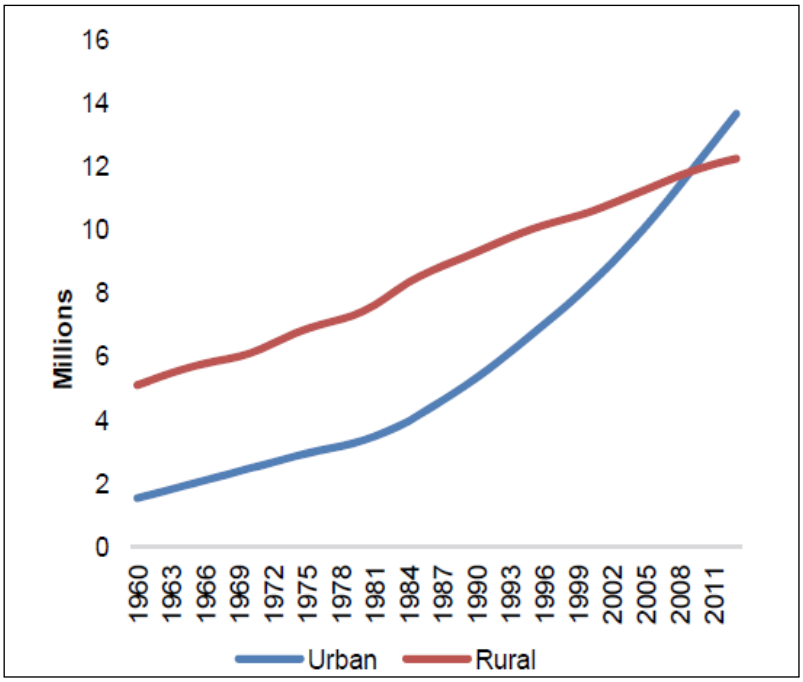

Figure 2. *Urban Population Growth Versus Rural Population Growth (Source: World Bank,2015)*

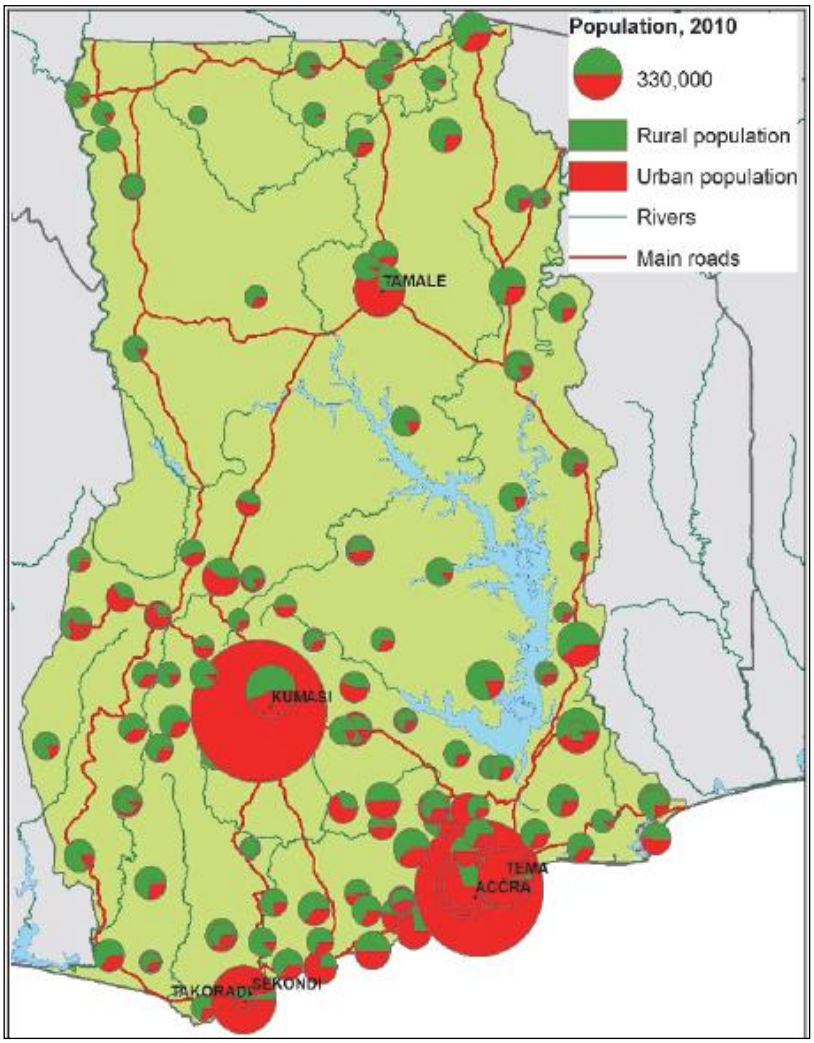

Figure 3. *Urban versus Rural Populations (2010) in Major Cities (Source: World Bank,2015*)

1.4 Climate in Ghana

Located in the tropical zone, Ghana has two distinctive climate seasons annually which are dominated by Inter-Tropical Convergence Zone (ITCZ) and the West African Monsoon (Stanturf et al., 2011). The first is the harmattan (dry) season which is caused by dry winds blowing from the Sahara to the Gulf of Guinea. This period lasts from late November till March in the south and May in the North (Asante and Amuakwa-Mensah, 2014). This period is characterized by cool and dry dusty winds with temperatures ranging from 27 °C to as high as 35 °C. The second major season is the wet or monsoon season, which is because of the southwest monsoon winds from the Gulf of Guinea. This period generally lasts from April to October and temperatures within the period can be as low as 24 °C and high as 29 °C. Northern Ghana has rain from about May to October while in Southern Ghana the rains last from April to July and again from September to November (Asante and Amuakwa-Mensah, 2014). The differences in the climatic conditions in the halves of the country underlie the division of the country into six ecological zones (Figure 4) namely; Sudan Savannah, Guinea Savannah, Forest Savannah Transition (Transitional zone), Semi-Deciduous Rainforest, Rainforest, and Coastal Savannah (Issaka et al., 2012). The Guinea Savannah zone and the Sudan Savannah covers the Northern Part whiles the coastal Savannah, Semi-Deciduous Rainforest, Rainforest, and Transitional zone cover the southern part.

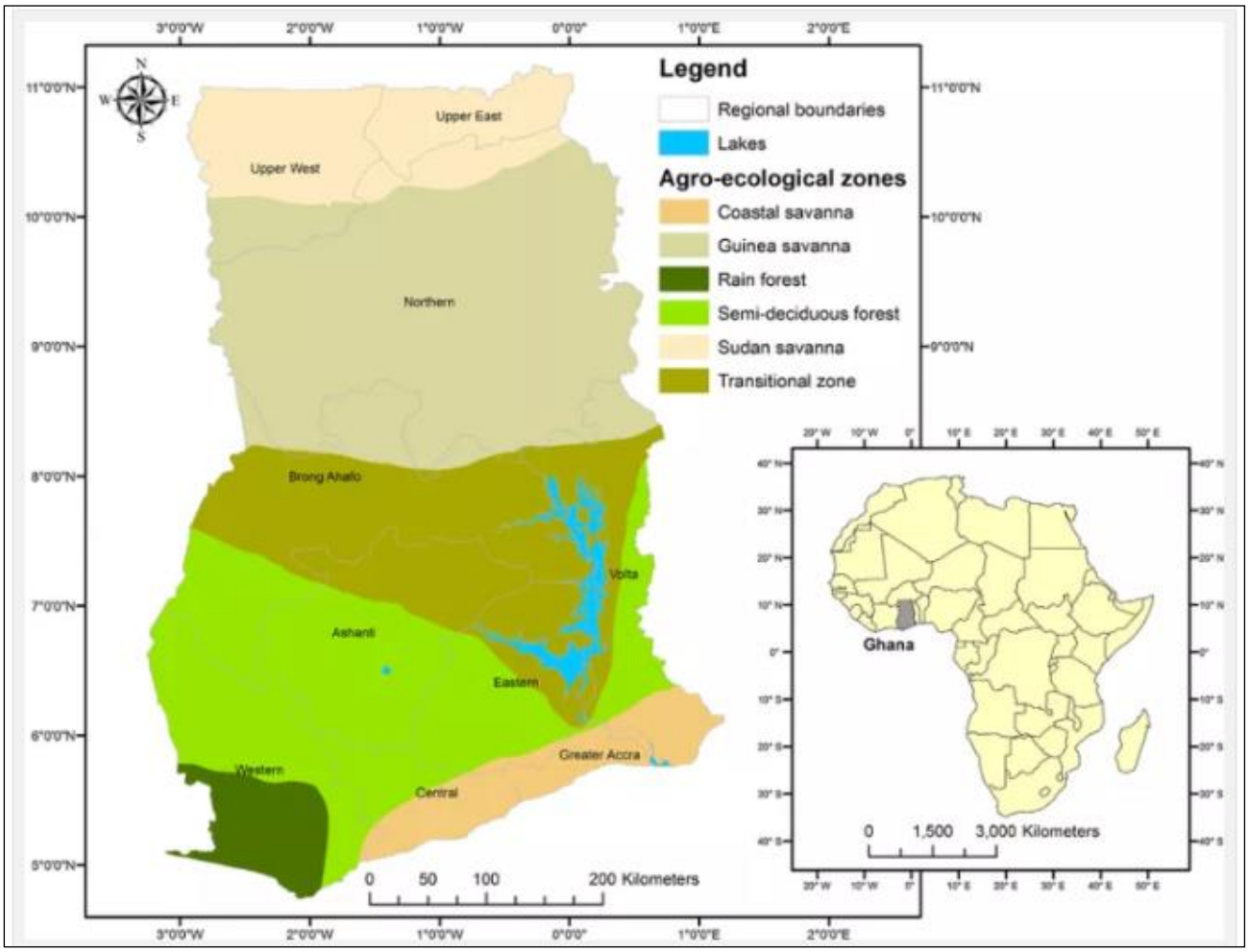

Figure 4. *Ecological Zones Map of Ghana (Source: www.agricinghana.com)*

1.4.1 Climate change in Ghana

"Climate change refers to any significant change in measures of climate (such as temperature, precipitation, or wind) lasting for an extended period" (US-EPA, 2008). According to the US-EPA (2008) climate change may result from natural factors (e.g. change in the Earth's orbit), natural processes within the climate system (e.g. changes in ocean circulation) or anthropogenic activities that change the atmosphere's composition (e.g. burning fossil fuels) and the land surface (e.g. deforestation, reforestation, or urbanization).

Available temperature data indicate a warming climate in Ghana with the northern area warming more rapidly than southern Ghana with a rise in mean annual temperature by 1.0°C since 1960 (Stanturf et al., 2011; Kankam-Yeboah, 2010). Stanturf et al (2011) from their analyses projected temperatures to rise by about 1.5 to 2.0 °C to about 3°C by 2080, also it is anticipated that changes in the ecological zones will be different. The change in Ghana's climate can be linked to factors like industrialization and urbanization (Manu et al., 2006). The overall greenhouse gases emission increase by 107% from 1990 to 2006 (Asante and Amuakwa-Mensah, 2014). According to Manu et al. (2006), between the years 1991 and 2000, the cities of Accra and Kumasi (Ghana's two largest cities) experienced a rise in average temperatures of 0.02 °C and 0.04 °C respectively. They further noted these rates as significant for these areas and concluded the rise resulted from anthropogenic heat and urbanization.

2. Data and methods

2.1 Data

This research employed datasets collected via sensors onboard Earth Observation Satellites (EOS). Landsat images were the main datasets for this research and were complemented by estimated atmospheric correction parameters from MODTRAN. Administrative boundaries and urban extents in shapefile formats were obtained from the Centre for Remote Sensing and Geographic Information Services – University of Ghana (CERGIS) were used to subset images to study areas.

2.1.1 Study areas

The limits for the study areas for this research are defined by generating a 5 km buffer around urban limits as shown in figures 5 and 6.

Accra is Ghana's capital and situated along the Gulf of Guinea on latitude 5° 33′ 0″N and longitude 0° 13′ 0″W (Manu et al., 2006). The city has a population of about 2,036,889 according to the Ghana Statistical Services (GSS). Acheampong et al. (2016) report that the city is growing at an annual rate of 4.2% which culminates in the rise of demand for housing. As the capital city, it is not spared from the influx of migrants from the rural areas who travel to seek greener pastures. Accra experiences two main seasons (dry and wet) with mean annual rainfall between 740 and 890 mm and temperature of 26.8^0 C (Manu et al., 2006; Ghana Statistical Services, 2014b). The limits of the study area for this research covers the Accra metropolis and the Tema metropolis.

Kumasi is Ghana's second largest city and located in the Ashanti Region lies on latitude 6° 41′ 0″N and longitude 1° 37′ 0″W (Cobbinah and Niminga-Beka, 2017). The city has a population of over 2,057,084 inhabitants according to the GSS. Originally designed as a garden city, it has gradually lost the right to be tagged as such given the massive influx of migrants which results in the spread of slum communities, urban sprawl and housing challenges (Cobbinah and Niminga-Beka, 2017; Mensah et al., 2018). Kumasi receives two rainfall seasons and a dry season with a mean rainfall of 1448mm and an average temperature of 26.3 º C (Ghana Statistical Services, 2014c). The limits of the study area for this research covers the Kumasi metropolis and some parts of adjoining municipalities.

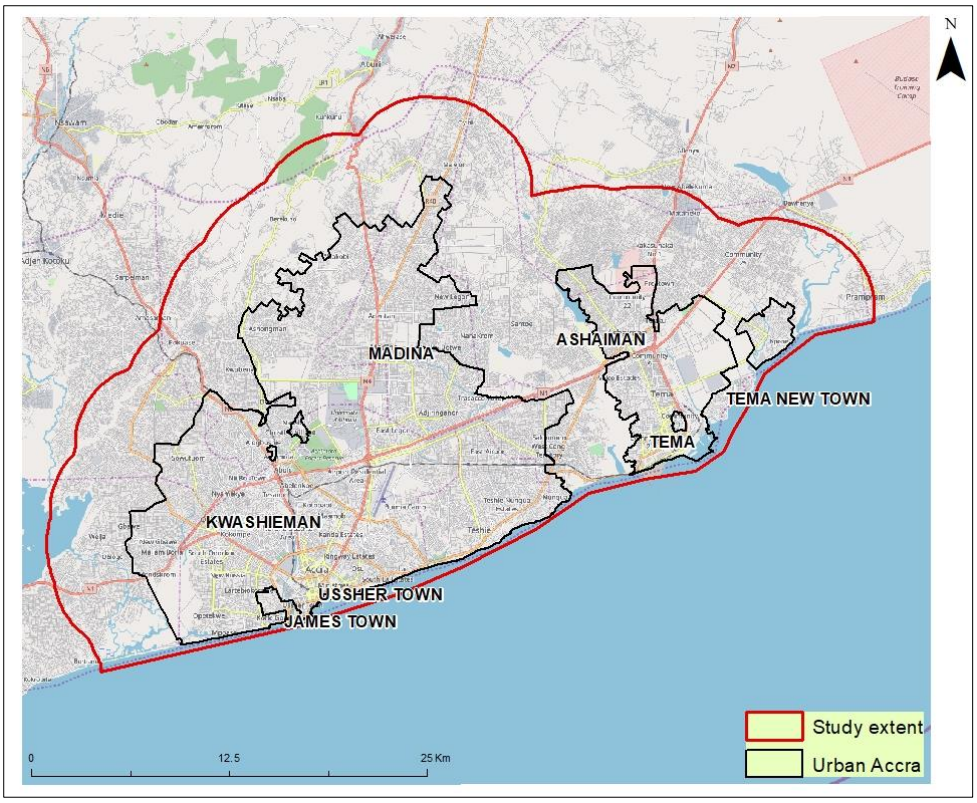

***Figure 5**. Study area map for Accra (basemap source: www.osm.com) black outline is the urban extent according to CERGIS*

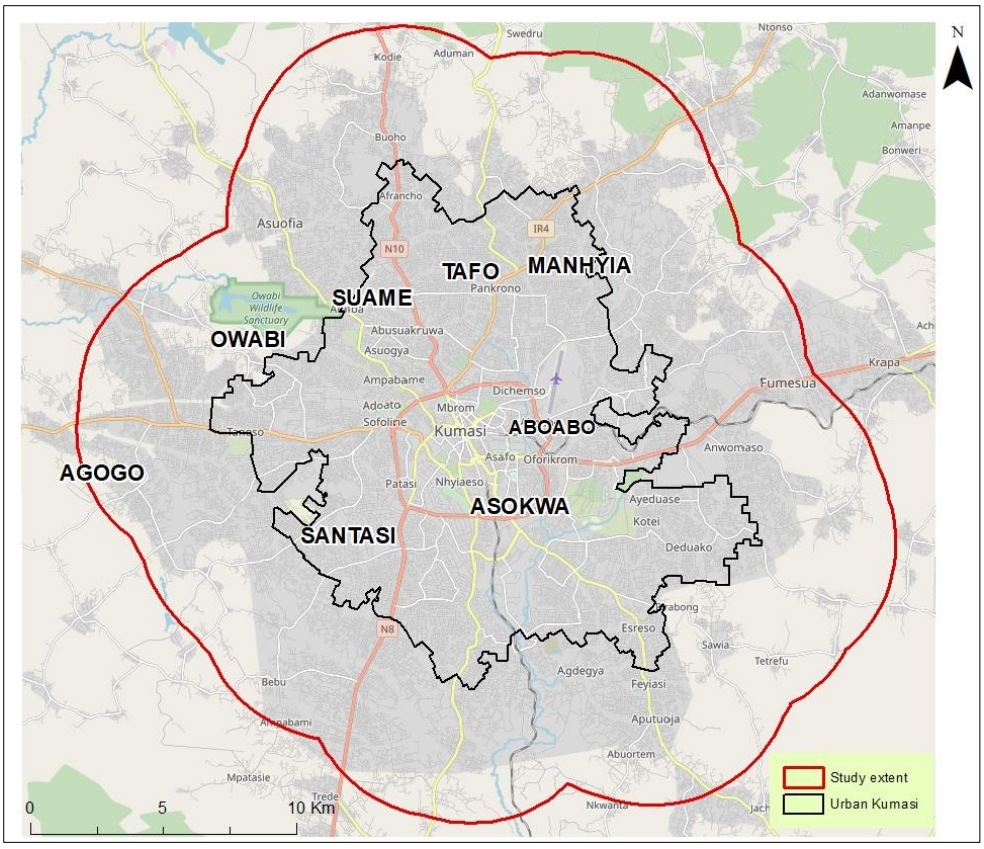

***Figure 6**. Study area map for Kumasi (basemap source: www.osm.com) black outline is the urban extent according to CERGIS.*

2.1.2 Satellite imagery

The National Aeronautics and Space Administration (NASA) in collaboration with the United States Geological Survey (USGS) has collected EOS images from different sensors aboard Landsat missions since 1972 (USGS, 2016). Landsat has seven different missions to its credit since its inceptions. The Landsat archive of EOS images from its six missions (the sixth mission failed to reach orbit) is arguably the largest database of its kind and the Landsat 5 is the longest provider of EOS images with records covering 28 years 10 months (USGS, 2016). Five different sensors have been deployed over different missions. The Multispectral Scanner (MSS) with the Landsat 1-3, Thematic Mapper (TM) with the Landsat 4, Enhanced Thematic Mapper plus (ETM+) with Landsat 7, Landsat 8 has two sensors which are the Operational Land Imager (OLI) and the Thermal Infrared Sensor (TIRS) (Loveland et. al, 2018). Images from missions from the fourth to the recent have thermal bands that are useful for the estimation of Land surface temperatures in addition to other bands recorded at wavelengths (Figure 7).

[OLI, Operational Land Imager; TIRS, Thermal Infrared Sensor; ETM+, Enhanced Thematic Mapper Plus; TM, Thematic Mapper; MSS, Multispectral Scanner; --, not applicable]

Band designations	Landsat band wavelength comparisons All bands 30-meter resolution unless noted									
	L8 OLI/TIRS		L7 ETM+		L4-5 TM		L4-5 MSS*		L1-3 MSS*	
Coastal/Aerosol	Band 1	0.43–0.45	--	--	--	--	--	--	--	--
Blue	Band 2	0.45–0.51	Band 1	0.45–0.52	Band 1	0.45–0.52	--	--	--	--
Green	Band 3	0.53–0.59	Band 2	0.52–0.60	Band 2	0.52–0.60	Band 1	0.5–0.6 *	Band 4	0.5–0.6 *
Panchromatic	Band 8**	0.50–0.68	Band 8 **	0.52–0.90	--	--	--	--	--	--
Red	Band 4	0.64–0.67	Band 3	0.63–0.69	Band 3	0.63–0.69	Band 2	0.6–0.7 *	Band 5	0.6–0.7 *
Near-Infrared	Band 5	0.85–0.88	Band 4	0.77–0.90	Band 4	0.76–0.90	Band 3	0.7–0.8 *	Band 6	0.7–0.8 *
Near-Infrared	--	--	--	--	--	--	Band 4	0.8–1.1 *	Band 7	0.8–1.1*
Cirrus	Band 9	1.36–1.38	--	--	--	--	* Acquired at 79 meters, resampled to 60 meters ** 15-meter (panchromatic) T1 = Thermal (acquired at 100 meters, resampled to 30 meters) T2 = Thermal (acquired at 120 meters, resampled to 30 meters)			
Shortwave Infrared-1	Band 6	1.57–1.65	Band 5	1.55–1.75	Band 5	1.55–1.75				
Shortwave Infrared-2	Band 7	2.11–2.29	Band 7	2.09–2.35	Band 7	2.08–2.35				
Thermal	Band 10 T1	10.60–11.19	Band 6 T2	10.40–12.50	Band 6 T2	10.40–12.50				
Thermal	Band 11 T1	11.50–12.51	--	--	--	--				

Figure 7. *Comparison of the bands and wavelengths landsat sensors (source: USGS)*

Landsat missions provide multispectral images with bands for classifications of land cover and the estimation of land surface temperatures (from TM, ETM and OLI sensors). Researchers like (Bouhennache et. al, 2014; Vittek et. al, 2014) have employed datasets from the missions in the detection of land cover while (Sagris and Sepp, 2017; Amer et al., 2017) utilized similar images for the estimation of land surface temperatures. In the estimation of LST, the water vapor content in the area of study is an important parameter. In situ measurements can be made to ascertain the values but data from MODIS presents an alternative (Cristóbal et. al, 2018). Other sources like the AERONET website provides accurate data for this parameter.

Table 1 provides a summary of the Landsat images by sensor and date of acquisition collected for this research. Landsat products downloaded from the Earth Explorer portal are named in the format LXSS_LLLL_PPPRRR_YYYYMMDD_yyyymmdd_CC_TX according to USGS (n.d) (*L = Landsat,X = Sensor, SS = Satellite, LLLL = Processing Correction Level, PPP = WRS Path RRR = WRS Row, YYYYMMDD = Acquisition Date, yyyymmdd = Processing Date, CC = Collection Number, TX = Collection Category*)

Table 1. Summary of Landsat Images Collected

Product	Sensor	Acquisition Date	Location
LE07_L1TP_193056_20021226_20170127_01	ETM+	26-12-2002	Accra
LE07_L1TP_193056_20110117_20161210_01	ETM+	17-01-2011	Accra
LC08_L1TP_193056_20170415_20170501_01	OLI/TIRS	15-04-2017	Accra
LE07_L1TP_194055_20020507_20170130_01	ETM+	07-05-2002	Kumasi
LE07_L1TP_194055_20100206_20161217_01	ETM+	06-02-2010	Kumasi
LE07_L1TP_194055_20171226_20180121_01	ETM+	26-12-2017	Kumasi

MODIS sensors on Terra and Aqua satellites are developed to collect global data for studying changes in land, oceanic, and atmospheric systems at a frequency of 1 to 2 days, in 36 spectral bands, or groups of wavelengths (Xiaoxiong et. al, 2009). NASA makes available raw data from the sensors such as aerosol data, water vapor, raw radiances as well as processed data in the form of land surface temperatures and NDVI datasets for free.

Although MODIS data serves as a good source of acquiring atmospheric parameters for the estimation of land surface temperatures, it is not possible to rely on products of the sensor when the interested in periods prior to its launch. Fortunately, the web-based tool MODTRAN designed by NASA provides the necessary parameters given the specifications (date of acquisition, geographic coordinates and sensor type) of a Landsat image (Barsi et al., 2003).

2.1.3 Vector datasets

Administrative boundaries of the study area and urban extents are necessary to subset the images to the extent of the study. This allows for the fast processing of images when using various algorithms. The data is in ESRI shapefile format and was obtained from CERGIS.

2.2 Methods

The research was conducted in three major phases to achieve the desired objectives. The first phase covered the collection of the relevant images for the study areas. Furthermore, the necessary pre-processing tasks to make them ready for analyses occurred in this phase. The Second phase focused on the computation of the desired spectral indices and generation of land cover and land surface temperature products/maps. Finally, the last phase concentrated on finding the nature of the sprawling phenomenon and the heat islands in the study area and ultimately the relationships between both. In addition, the final phase saw a calculation of an urban expansion rate and a heat island intensity for each study area. Figure 8 provides a summary of the workflow.

***Figure 8**. Flowchart of methods*

2.2.1 Image collection and pre-processing

Images for this project are acquired from Earth Explorer, the online portal of the USGS which hosts a myriad of remotely sensed products and other derivatives from NASA. Landsat images (with thermal bands) were downloaded by entering the study area name and specifying a date range. The product type was set as Landsat level 1 product whiles all other criteria remained default. The portal allows users to define other specifications like the percentage of cloud cover and time of the day. In this case, the goal was to manually inspect each product to assess their appropriateness by setting small date ranges. Corresponding atmospheric correction parameters were obtained using NASA's Atmospheric Correction Parameter Calculator (MODTRAN).

Despite the corrections made to the original Landsat products to upgrade it to level 1, some further corrections were applied given the objectives of the project. Electromagnetic energy recorded by sensors is influenced by particles in the atmosphere such as aerosols through scattering or absorption (López-Serrano et al., 2016, Bakker et al., 2001). For this purpose, the Fast Line-of-sight Atmospheric Analysis of Spectral Hypercubes (FLAASH) in the ENVI software was used. FLAASH is a first-principles atmospheric correction methodology based on MODTRAN which is incorporated in the ENVI software package (Matthew et al., 2002). Subsets of the corrected images were made to cover the study areas.

2.2.2 Land cover and land surface temperature products

To characterize the phenomenon of sprawl and appreciate its effects of UHI in the study areas, two derivatives were generated from the satellite images using some well-known indices. The derivatives were land cover and LST products.

Derivation of land surface temperature

Land surface temperature products were derived by using the Single-Channel (SC) algorithm developed by Sobrino and Jiménez-Muñoz (Sobrino and Jiménez-Muñoz, 2010). The SC method is one of many algorithms for the estimation LST, others include the Split-Window, the Dual Angle Algorithm and the Radiative Transfer Equation-Based Method (Sagris and Sepp, 2016; Yu et al.2014). Landsat sensors TM and the EMT+ record thermal information in a single band which makes the SC algorithm suitable for deriving LST products from their images (Yu et al., 2014, Sobrino and Jiménez-Muñoz, 2010). A successful application of the SC algorithm depends on the availability of atmospheric functions computed from water vapor content values and land surface emissivity (Jiménez-Muñoz et al., 2009, Sobrino and Jiménez-Muñoz, 2010). The SC is given by equation (1) according to Sobrino and Jiménez-Muñoz (2010):

$$T_s = \gamma \left[\frac{1}{\varepsilon} (\psi_1 L_{sen} + \psi_2) + \psi_3 \right] + \delta \quad (1)$$

Where L_{sen} is the at-sensor radiance in W $m^{-2}sr^{-1}$, ε is the surface emissivity, γ and δ are two parameters dependent on the Planck's function, and ψ1, ψ2, and ψ3 are the atmospheric functions (Sobrino and Jiménez-Muñoz, 2010).

Emissivity values are estimated from algorithms like the Classification-based Emissivity Method (CBEM), NDVI-based emissivity method, and day/night Temperature-Independent Spectral-Indices (TISI) based method (Yu et al., 2014). The NDVI approach is considered for this research. This approach is a three-step process that first involves the calculation of NDVI, estimation of Fractional vegetational cover and ultimately emissivity values based on NDVI thresholds (Sobrino et al., 2004; Sagris and Sepp, 2016). NDVI is calculated by equation 2 (Sagris and Sepp, 2016):

$$NDVI = \frac{\rho_{nir} - \rho_{red}}{\rho_{nir} + \rho_{red}} \quad (2)$$

Where NIR and red are the Near-Infrared and Visible Red bands respectively. The fractional vegetational cover is calculated using equation 3 (Jiménez-Muñoz et al., 2009)

$$FVC = (NDVI - NDVI_{soil}) / (NDVI_{veg} + NDVI_{soil}) \quad (3)$$

NVDI of soil is given as 0.2 and vegetation as 0.5 (Sobrino et al., 2004; Yu et al., 2014; Sobrino and Jiménez-Muñoz, 2010; Sagris and Sepp, 2016). Finally, the emissivity for soil, vegetation and, mixed classes are calculated using equation 4 (Sagris and Sepp, 2016)

$\varepsilon = \varepsilon_s * (1\text{-}FVC) + \varepsilon_v * FVC$ (4)

ε_s and ε_v are emissivity values for soil and vegetation estimated at 0.97 and 0.99 respectively (Sobrino et al., 2004). Atmospheric Functions (AF) ψ1, ψ2, and ψ3 are calculated by equation 5 (Sagris and Sepp, 2016 and Jiménez-Muñoz et al., 2009)

$$\begin{bmatrix} \psi_1 \\ \psi_2 \\ \psi_3 \end{bmatrix} = \begin{bmatrix} c_{11} & c_{12} & c_{13} \\ c_{21} & c_{22} & c_{23} \\ c_{31} & c_{32} & c_{33} \end{bmatrix} \begin{bmatrix} w^2 \\ w \\ 1 \end{bmatrix} \quad (5)$$

Where w is the water vapor content and coefficients c_{ij} are obtained from simulated data constructed from atmospheric profiles included in different databases and MODTRAN4 radiative transfer code (Sobrino and Jiménez-Muñoz, 2010). AF can also be computed directly from MODTRAN upwelling and downwelling estimations using the relationships in equation 6 (Sobrino and Jiménez-Muñoz, 2010):

$$\psi_1 = \frac{1}{\tau} \quad \psi_2 = -L^{\downarrow} - \frac{L^{\uparrow}}{\tau} \quad \psi_3 = L^{\downarrow} \quad (6)$$

where τ is the atmospheric transmissivity, $L\uparrow$ is the upwelling atmospheric radiance, and $L\downarrow$ is the downwelling atmospheric radiance (Yu et al., 2014).

Parameters from Planck's function γ and δ are computed using equations 7 and 8 respectively according to Sobrino and Jiménez-Muñoz (2010):

$$\gamma \approx \frac{T_{sen}^2}{K_2 L_{sen}} \quad (7)$$

$$\delta \approx T_{sen} - \frac{T_{sen}^2}{K_2} \quad (8)$$

T_{sen} represents the at-sensor brightness temperature which is calculated using equation 9 (Sobrino and Jiménez-Muñoz, 2010):

$$T_{sen} = \frac{K_2}{\ln\left(\frac{K_1}{L_{sen}} + 1\right)} \quad (9)$$

K_1 and K_2 are thermal band constants provided in the metadata of the image.

Classification of built-up area

Land cover products generated for the study areas for their respective years provide empirical evidence to identify the rate of urban growth and subsequently urban sprawl (Inostroza et al., 2019). The classification process was initiated by multiresolution segmentation followed by a spectral difference segmentation. The segmentations were based on spectral values of the bands of the atmospherically corrected images and their built-up index layers in eCognition. The built-up index layer was generated for each image using equation 12. Layers such as the built-up index layer, and the bands relevant for computing the spectral indices were assigned higher weights for the segmentation. Landscapes are made of different homogeneous parts and patterns commonly referred to as patches (Antrop,2018; Blaschke and Strobl,2001). These patches are made up of several pixels which are the basic units in images. Therefore, Blaschke and Strobl (2001) point out that it is appropriate to perform statistical analysis on patterns than individual pixels for built-up areas. By performing an image segmentation, meaningful image objects are generated which can be classified and are representations of the patches in the real world (Baatz & Schäpe, 2010). Image objects are essentially spatially clustered pixels that have high spectral autocorrelation since they are part of the same object (Hay et al., 2003).

Spectral indices NDWI, VrNIRBI, NDVI, NDBI, and DBSI were computed as customized object features. The NDWI which stands out as the best spectral index for extraction of water bodies was used. The index is calculated based on the Near-Infrared band (NIR) and the green band of the Visible region of the Electro-Magnetic Spectrum (Rokni et al., 2014). Water absorbs radiations in the NIR region whiles vegetation will reflect such radiations hence appropriate for computing the index (Rokni et al., 2014). NDWI is calculated by the equation 10 (Rokni et al., 2014):

$$NDWI = \frac{Green - NIR}{Green + NIR} \tag{10}$$

The Visible red Near-Infrared based Built-up Index (VRNIR-BI) proposed by Estoque and Murayama (2014) was computed and assessed as a built-up index for extracting built-up areas given it is considered a more robust index compared to other similar indices like NDBI. VrNIR-BI is calculated by equation 11:

$$\text{VrNIR-BI} = \frac{\rho_{\text{Red}} - \rho_{\text{NIR}}}{\rho_{\text{Red}} + \rho_{\text{NIR}}} \tag{11}$$

Where NIR and Red are the Near-Infrared and Red bands respectively. Nonetheless, the NBDI (Rasul et al, 2018) given by equation 12 was also computed to assess how both indices fared for the study areas.

$$\text{NDBI} = \frac{\rho_{\text{SWIR1}} - \rho_{\text{NIR}}}{\rho_{\text{SWIR1}} + \rho_{\text{NIR}}} \tag{12}$$

An additional index, the Dry Bare-Soil Index (DBSI) suggested by Rasul et al. (2018) was computed to facilitate the delineation bare lands which also tend to have high values of NDBI. The index is computed by equation 13.

$$DBSI = \frac{\rho_{SWIR1} - \rho_{Green}}{\rho_{SWIR1} + \rho_{Green}} - NDVI \tag{13}$$

Upon initial assessments, the VrNIR-BI was excluded in further processes for several reasons which are discussed in the results section.

An initial classification which separated image objects into built-up, non-built-up and water was achieved by a sample-based classification using a Support Vector Machine (SVM) algorithm in eCognition. Training for the classification was based on the mean layer values and the indices of the image objects for each image.

Five new classes (high urban density, low urban density, bare soils, vegetated, and sparsely vegetated) were created. Objects were reassigned to these classes using a rule-based classification approach. Rules were generated in eCognition based on spectral indices values and locations of objects as well as expert knowledge. The classes high urban density and low urban density were created as subclasses for the built-up area whereas the classes vegetated lands, bare soils and sparsely vegetated lands were created as subclasses for the non-built-up class.

The final classified image objects were visually verified in Google Earth Pro by backdating images to respective years since enough ground-truth data was unavailable.

2.2.3 Assessment of phenomena

The third and final phase of this methodical approach focused on the assessment of the two phenomena under consideration and how they relate to each other for the study areas.

The land cover changes were assessed by a spatial union of all three resulting layers of the respective study areas. The net process was classified based on the resulting combinations of the land cover type from each year.

Finally, the SUHI intensity (SUHII) was calculated by way of finding the difference in mean temperatures urban and rural (Li et al.2018). This was achieved by dissolving the polygons (classified image objects) based on their classes and finding the mean LST for each class using zonal statistics. The mean temperatures for all built-up and non-built-up classes were calculated to determine the SUHII. The hottest region analysis was done using the Surface Urban Heat Island Magnitude (SUHIM) approach which is based on statistical normalization of LST. (Schwarz et al. 2011, Sagris and Sepp, 2016). Using zonal statistics and map algebra it is possible to define a threshold that could be used to separate the hottest region from other parts within a study area. This implies that different values can be employed based on different criteria. For this research, the sum of the mean and standard deviation (mean + std) was used as the threshold following Sagris and Sepp (2016).

3. Results

3.1 Land cover

The land cover was categorized into six classes that are representative of the nature of the landscape of the study areas. The built-up (urban) cover divided into two subclasses allowed for the identification of lowly and highly dense urban patches within the study areas. In a similar fashion, non-built-up lands were divided into three subclasses (vegetated, sparsely vegetated and bare soil). They set the tone to assess the impact of the heat island for various cover types. Due to the low level or absence of vegetation, the bare soil class had high values in the NDBI, as built-up areas did. To distinguish them DBSI was used. Similarly, the sparsely vegetated areas had a spectral collision with low-density urban space: NDVI values are in between vegetated and non-vegetated. Classification using both NDVI and NDBI made it possible to distinguish them. These patches are usually open fields with a mix of bare soil and unhealthy vegetation that are used for various purposes. Some examples are grazing pastures, small to medium scale farms, poorly conditioned sports grounds and deforested areas that are yet to be developed for real estate purposes. These sparsely vegetated patches are predominantly the transition zones from vegetated patches to urban. Vegetated patches, on the other hand, are mostly dense forests, large farms or natural reserves.

Dynamics in land cover classes are presented in table 2 (in absolute numbers, ha) and in percentage in figures 9 and 10. It is evident that in Accra the area of urban space increased by 22843 ha and by 6925 ha by 2011 and 2017 respectively. That makes 2538 ha per year before and 1154 ha per year after 2010. In percentage terms, the growth was 70.3% and 12.5% for pre-2011 and post 2011 periods respectively. By 2010, low-density urban areas grew larger than high-density areas. But had a reduction in the area by 2017 which suggests some of the low-density areas became densified (Table 2).

Urban space increased by 9473 ha and 6064 ha by 2010 and 2017 respectively in Kumasi with growth pace of 1184 and 866 ha per year accordingly. In the two periods, the city expanded by 85.4% and 29.5% correspondently. High-density areas grew larger than low-density areas.

In Accra, all non-built-up areas made significant losses over the study period whiles the built-up patches continued to make significant gains based on values in table 2. Non-built-up areas decreased from 75111 ha to 45343 ha or by 39% for the whole period. In effect, the non-built-up areas in Accra became built-up at a rate of 1934 ha per year. Bare soils were the main land cover class in rural space overtaken by urban sprawl. Direction wise, the expansion predominantly approached the western side and so was the densification as depicted in the land cover map (Figure 11). Meanwhile, in Kumasi, a different pattern was noticed. While bare soils and vegetation made losses, the built-up areas, sparsely vegetated areas, and water bodies made gains over the period. By 2017, sparsely vegetated areas increased by 27431 ha causing its total area to change from 9100 ha to 36532 ha. Although water bodies made some gains of about 25 ha, it is assumed the value would have been lesser had it not been for cloud cover over the Owabi dam in the image for 2002. Despite this, it is evident from figure 11 that some man-made ponds sprung up in the area by 2017. The sprawl was even in all directions as seen in figure 11.

The land cover maps (Figure 11) show that the aforementioned changes occurred in both areas. It is evident that all cover types experienced notable changes but for water bodies, which fairly maintained their fraction as shown in figures 9 and 10. In figure 10, the bare soils and water bodies are not represented as their percentages are less than 1%.

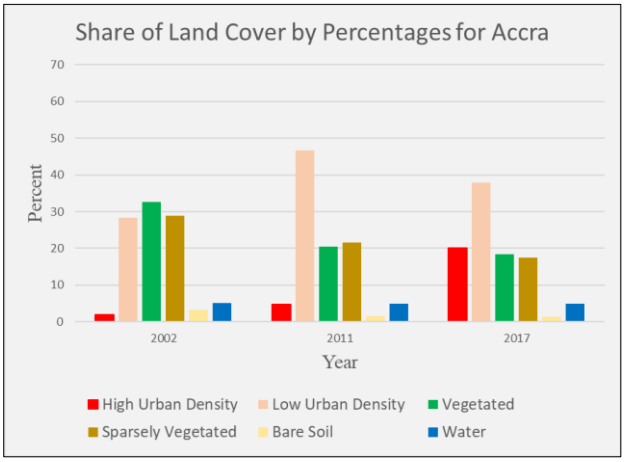

Figure 9. *Land cover share for Accra*

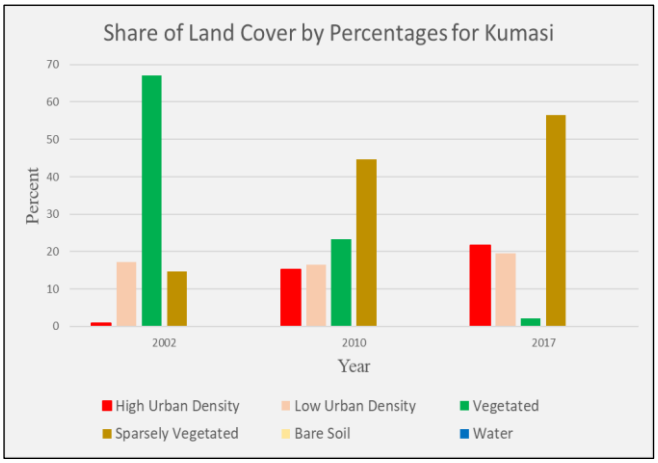

Figure 10. *Land cover share for Kumasi*

Table 2. Areas covered by Land Cover Classes

Accra (area/ha)			
Land Cover	**2002**	**2011**	**2017**
High Urban Density	2018	5160	21553
Low Urban Density	30453	50154	40686
Bare Soil	3434	1590	1494
Sparsely vegetated	30981	23217	18766
Vegetated	35184	22092	19803
Water	5513	5369	5280
Total	107582	107582	107582
Kumasi (area/ha)			
Land Cover	**2002**	**2010**	**2017**
High Urban Density	511	9872	13989
Low Urban Density	10585	10698	12645
Bare Soil	79	49	42
Sparsely vegetated	9100	28876	36532
Vegetated	41308	15076	1358
Water	53	74	78
Total	61637	64644	64644

* The difference in total area for Kumasi between the year 2002 and the rest of the years is because of cloud covered areas that were eliminated from the analysis.

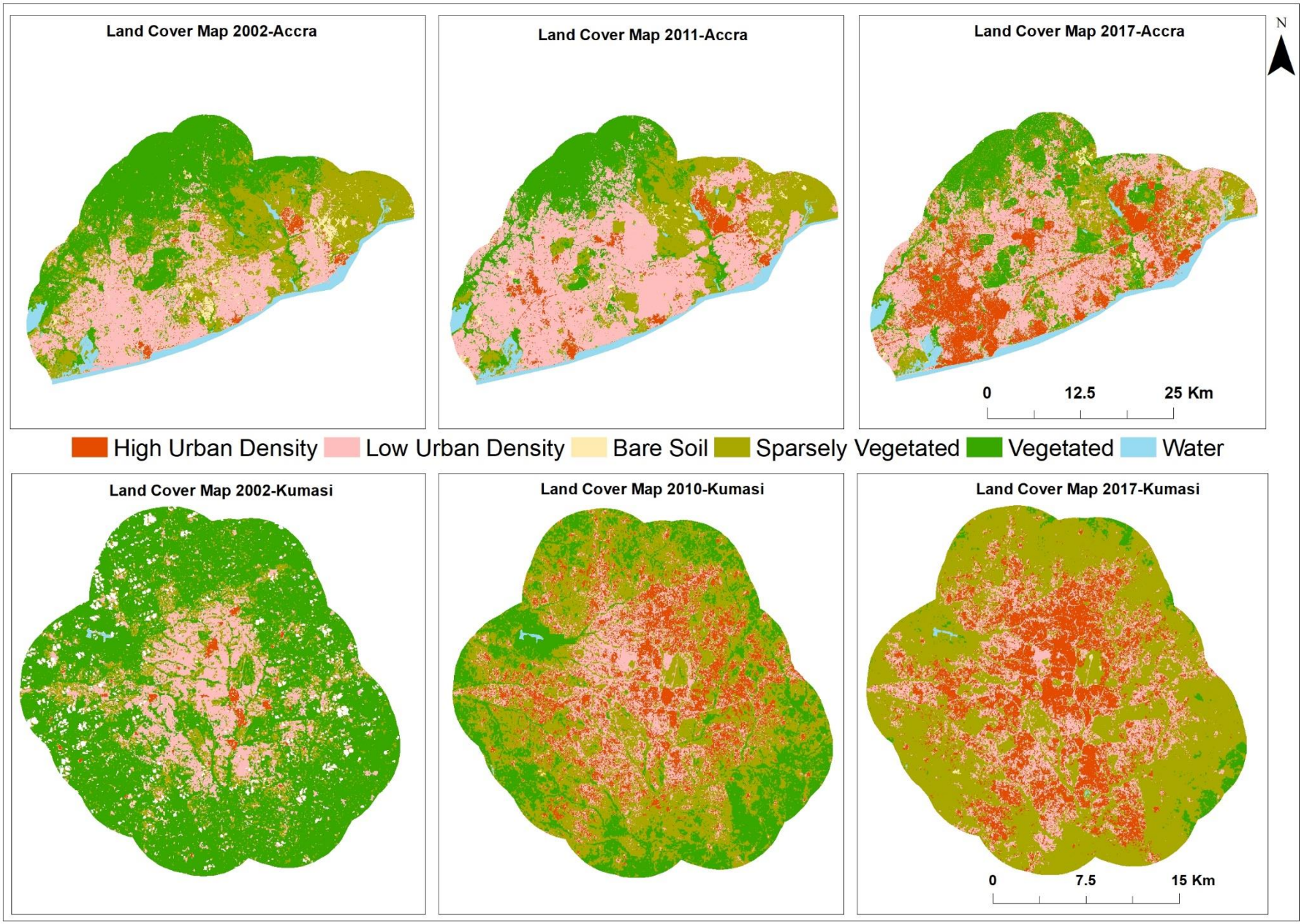

Figure 11. *Land cover maps*

3.2 Urban processes

Relevant to this research was how non-urban patches become urban and how existing urban areas changed over the course of time in terms of density and extent. Apart from the pace of urban sprawl, which can be estimated from results in section 3.1, it was interesting to identify the urban processes that the cities experienced. The processes which are noticed to have occurred over the period of investigation were labeled or classified as shown in table 3. The year 2002 was considered as the base year for both cities whiles the middle of the period was 2011 and 2010 for Accra and Kumasi respectively. The final year for both cities was 2017.

Table 3. Classifications of Urban Process

Cover Class, 2002	Process	Process Label
High Urban Density	Remained the same	High-Density Urban Core
Low Urban Density	Remained the same	Low-Density Urban Core
Low Urban Density	Became high density by the middle of the study period	ED - Early Densification
Low Urban Density	Became high density by the end of the study period	LD -Late Densification
Non-built-up	Became urban by the middle of the study period	EU -Early Urbanization
Non-built-up	Became urban by the end of the study period	LU -Late Urbanization
Non-built-up	Became urban and later densified	EU-LD -Early Urbanization with Late Densification
Non-built-up	Remained the same	NA

There were also process between built-up and non-built-up, which were difficult to explain (others) They correspond to 7% of the area in Accra and 6% in Kumasi region.

Table 4. Areas Covered by Urban Processes

Urban Processes	Accra (ha)	Kumasi (ha)
High-Density Urban Core	937	624
Low-Density Urban Core	15132	3145
ED - Early Densification	1877	3164
LD -Late Densification	11194	2717
EU -Early Urbanization	15343	6572
LU -Late Urbanization	12652	7884
EU-LD - Early Urbanization with Late Densification	4077	1828
NA	37937	34480
Others	8433	4230

The high-density urban core in Accra was found to be 937 ha (Table 4) which accounted for 0.9% of the total area. The low-density urban core in Accra covered a total area of 15132 ha which translates to 14.1% of the total area.

The urban densification process in Accra over the entire period covered a total area of 13071 ha. It was interesting to find out at what stage within the study period the process was great. Hence the process was categorized into two, based on the period by which the densification had occurred. Densification which took place by 2011(early densification) in Accra covered an area of 1877 ha which corresponds to 1.7% (Table 4). By 2017, an additional area of 11194 ha was densified and accounted for 10.4% of the total area (Table 4). Evidently, much of the densification process took place in the later part of the study period. Similarly, the urbanization process was categorized into two classes. The places that became urban by the year 2011, covered an area of 15343 ha representing 14.3%, while those that were later urbanized covered 12652 ha representing 11.8% (Table 4). Some of the areas that were urbanized by 2011, as low-density areas in Accra became high-density areas by 2017 accounted for 3.8% of the area with 4077 ha (Table 4). These areas were categorized as early densification with late urbanization.

In the case of Kumasi, the high-density urban core made up 1% of the entire area, which is 624 ha. The low-urban density core areas covered 3145 ha represented 4.9% of the total area. The densification process in Kumasi by 2010 covered 3164 ha which is approximately 4.9% (Table 4). By 2017, an area of 2717 ha had been densified in addition which represented 4.2%. Non-urban areas that became urban by 2010 and were categorized as early urbanized areas summed up to 6572 ha accounting for 10.2% while those that became urbanized in 2017 represented 12.2% with an area of 7884 ha. Early urbanized areas that were later densified represented 2.8% of the total area with a value of 4230 ha (Table 4).

In both areas, the urbanization was the leading process. It is worth noting that both densification processes in Kumasi covered approximately the same area in both periods while in Accra the later densification outweighed the early densification process.

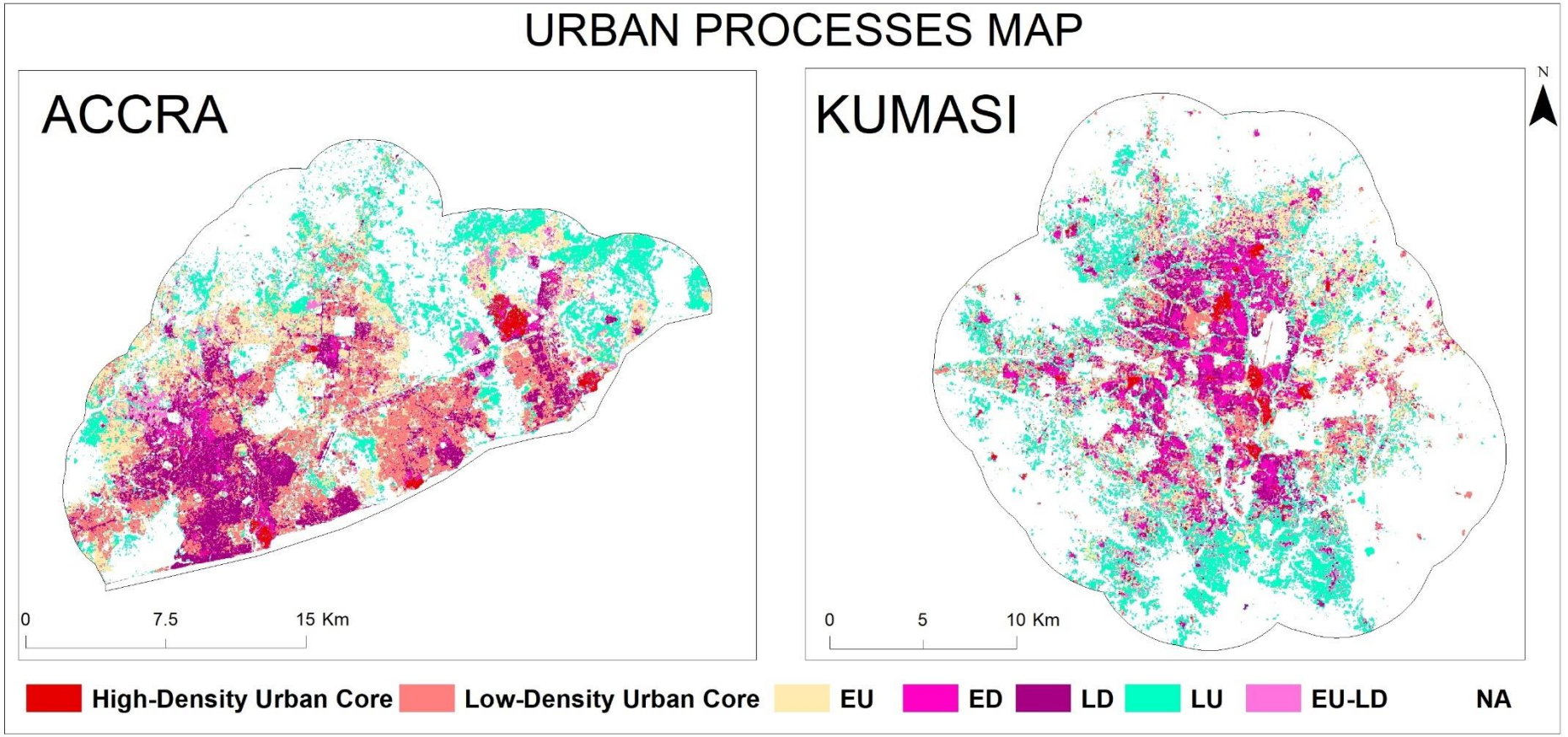

Figure 12. *Urban Process (EU-Early Urbanization, ED - Early Densification, EU-LD - Early Urbanization with Late Densification, LD-Late Densification, and LU -Late Urbanization) Maps.*

3.3 Land surface temperature

The land surface temperature (Figure 13) in both cities had values that fall within the range of expected values for the study areas. In 2002 for Accra and 2010 for Kumasi, there were some high values that are beyond the mean measured air temperature for Accra and Kumasi (Table 5). The relationship between the two measurements is that solar radiation heats up the ground object and their emitted heat contributes to the increase of air temperature. But there were still some anomalies of high and low values that are either above or below the temperature ranges for both areas.

Table 5. Mean Air Temperature, Mean LST mean, LST Standard Deviations and Anomalies

City	Date	Air Temp. mean (°C)	LST mean (°C)	LST std (°C)	Min anomaly (°C)	Max anomaly (°C)
Accra	26/12/2002	27.2	26.21	1.68	14	46
Accra	17/01/2011	27.2	26.8	1.98	17	
Accra	15/04/2017	28.1	26.71	1.61		
Kumasi	07/05/2002	26.3	23.92	1.46	18	
Kumasi	06/02/2010	29.6	30.82	2.48		55
Kumasi	26/12/2017	26.1	24.65	1.51		

The variations in the temperatures can be attributed to the different times of the year the images were acquired. Secondly, meteorological conditions for certain days also accounted for variations with an example being the day in 2010, which was an extremely hot day in Kumasi. The records from the National Oceanic and Atmospheric Administration (NOAA) climate data portal suggest the said day was extremely warm and part of a series of warm days (10 days) in the month of February. The average daily temperature for those days was 28.75 °C. Generally, the LST values do correlate with air temperature values (Table 5).

Assessing the land surface temperature with respect to the land cover reveals the influence of the individual cover types on the land surface temperature. By performing a zonal statistic operation in a GIS, the mean land surface temperature values for each land cover class was obtained (Table 6). In general, water had the lowest surface temperature for both areas which was followed by the vegetated cover.

Temperatures for high-density urban space were always higher than ones of low-density for both areas. The largest difference in Accra was in the year 2017, where the high-density area was warmer by 1.07 °C (Table 6). The differences for the other years were found to be less than 0.5 °C. In the case of Kumasi, there was a relatively bigger difference between the urban subclasses in 2002, where the high-density area was 1.95 °C warmer than the low-density area. The difference was lesser and fairly remained the same with 0.50 °C and 0.56 °C for the years 2010 and 2017 respectively (Table 6). Irrespective of the fact that these values may feel small, they are essential when considering the influence of land cover on surface temperature.

For non-built up cover types, bare soils had the highest surface temperatures of all the subclasses followed by sparsely vegetated areas, vegetated areas and water bodies for both cities. The bare soils did have higher temperatures because of the absence of vegetation. Comparing the temperatures of vegetated and sparsely vegetated areas in table 6, it is noticed that the sparsely vegetated areas are warmer than the vegetated.

In Accra, bare soils and sparsely vegetated areas were warmer than both urban areas in 2002 and 2011. Unlike sparsely vegetated areas in Accra, sparsely vegetated areas in Kumasi were less warm the urban

areas which could be attributed to healthy vegetation even though they had relatively lower NDVI. Bare soils in Kumasi were warmer than the low-density urban area for all three years and had values close to that of the high-density area as seen in table 6. The greatest difference between bares soils and the high-density urban patches was in 2002 where bare soils were 1.18 °C less warm.

Table 6. Mean surface temperature for Land Cover Classes

Accra (Mean Temperature, °C)			
Land Cover	**2002**	**2011**	**2017**
High Urban Density	27.38	27.74	28.16
Low Urban Density	27.13	27.35	27.09
Bare Soil	28.33	28.13	26.72
Sparely Vegetated	27.67	28.15	26.4
Vegetated	24.51	24.83	25.66
Water	22.09	22.62	22.78
Kumasi (Mean Temperature, °C)			
Land Cover	**2002**	**2010**	**2017**
High Urban Density	27.61	33.26	26.17
Low Urban Density	25.66	32.76	25.61
Bare Soil	26.43	33.51	26.32
Sparely Vegetated	24.48	30.75	23.83
Vegetated	23.3	28.03	22.38
Water	21.69	26.42	22.89

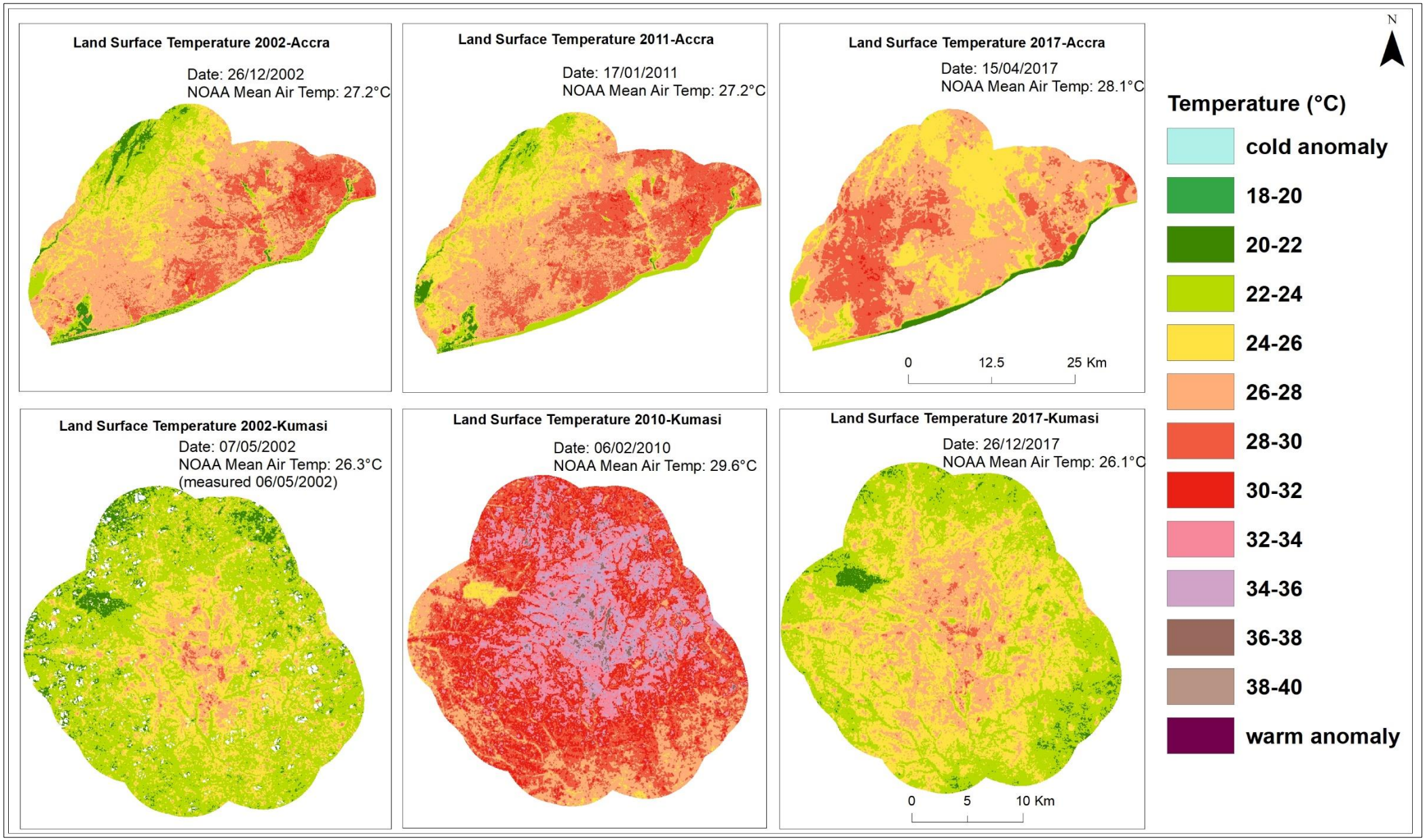

Figure 13. *Land surface temperature maps.*

3.4 Urban heat islands

To identify the spatial extent of the urban heat islands in the study area, the land surface temperatures were normalized to reduce the seasonal meteorological differences and effects of anomalies by finding the zonal mean temperature for the areas and the standard deviations. The land surface temperatures products were classified to identify heat islands as areas above the sum of mean temperature and the standard deviation (Figure 14).

The heat island effect was assessed in two ways. The first one considered the influence of the land cover types. The second approach separated the study areas into two classes, which were areas that had temperatures above the sum of the mean and the standard deviations (Table 5) and areas that did not.

The SUHI intensity based on land cover types is computed by finding the difference between mean surface temperature for built-up and non-built-up patches. For this purpose, an average of the mean temperatures for the non-built-up areas in table 6 was determined as well as one for the built-up areas. The intensities for the respective years are shown in table 7. It is evident that Accra the intensities increased over the past 15 years. The difference between the intensities of 2011 and 2002 was about 0.01 °C. Between 2011 and 2017, the difference in intensity was 0.62 °C.

The intensity on the urban-rural scale for Kumasi had a value of 2.66 °C and a value of 3.3 °C for 2010. The intensity for the year 2017 was 2.03 °C which was 1.3 °C less than the value for 2010. The high value in 2010 could come from attributed to the fact that the said day was an extremely hot day as already mentioned.

Table 7. Surface Urban Heat Island Intensities (SUHII)

City	SUHII, °C 2002	SUHII, °C 2010 – Kumasi/2011 -Accra	SUHII, °C 2017
Accra	1.60	1.61	2.24
Kumasi	2.66	3.33	2.03

Table 8. Surface Urban Heat Island Magnitude (SUHIM)

City	SUHIM, °C 2002	SUHIM, °C 2010 – Kumasi/ 2011 – Accra	SUHIM, °C 2017
Accra	3.43	3.02	2.66
Kumasi	2.93	4.42	2.8

The SUHIM, computed from the classified normalized land surface temperatures as seen in table 8 gave results that were different from the SUHII. In Accra the magnitude for 2002 was 3.43 °C while 2011 and 2017 were 3.02 °C and 2.66 °C respectively. In Kumasi, the magnitude for 2002 was 2.93 °C whiles 2010 and 2017 were 4.42 °C and 2.8 °C. The effect of the extremely hot day in Kumasi is clearly seen in the value of both intensities.

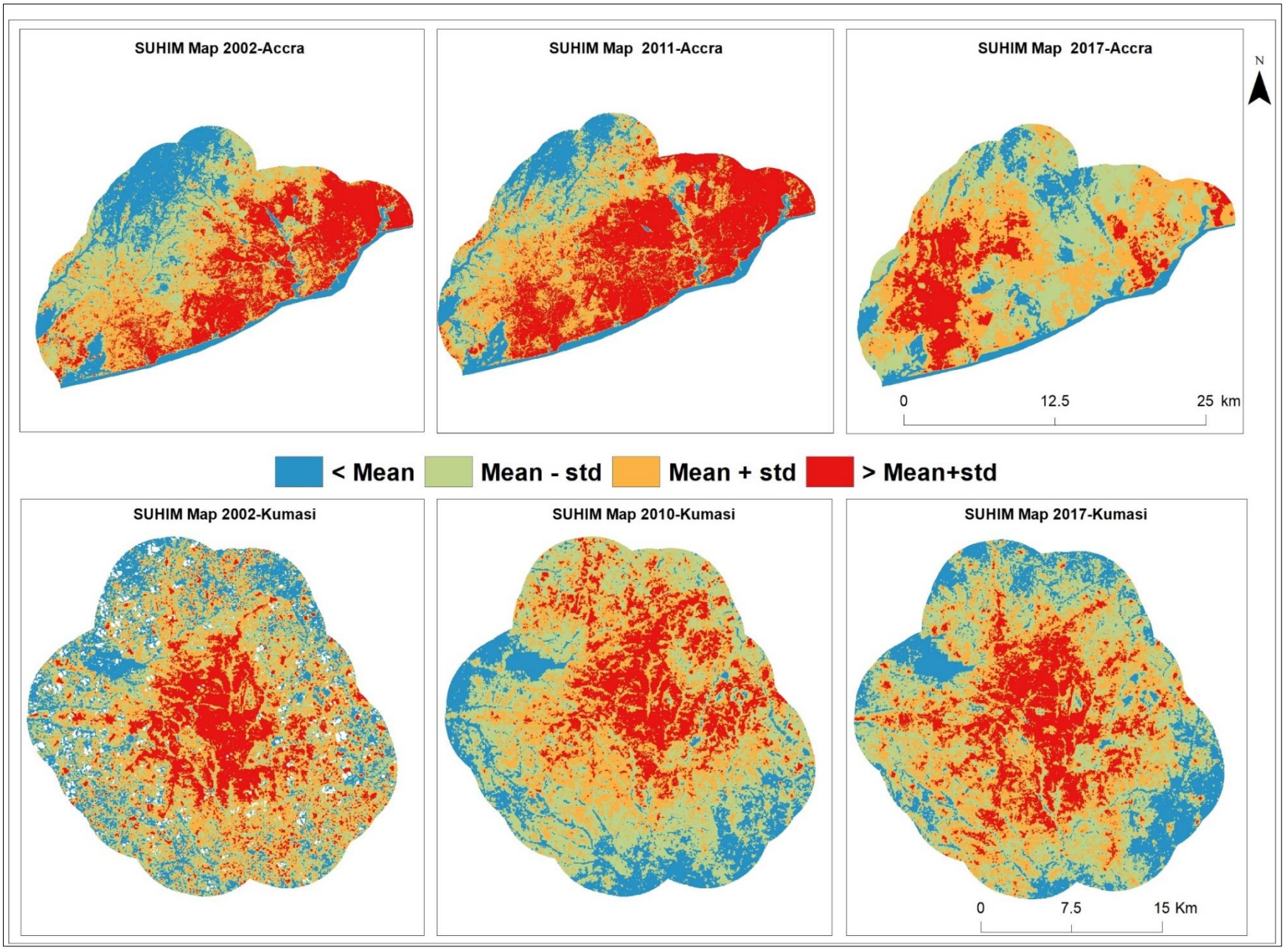

Figure 14. *UHI maps*

4. Discussion

4.1 Land cover classification

From a review of the literature, successful detection of urban sprawl is dependent on the classification of land cover. It is important to distinguish between built-up and non-built-up to achieve the detection and measurement of the phenomenon. This also helps in the detection of UHI and the calculation of its intensity. In this research, this was achieved by using EOS data, which is the most common data source for the task. The approach was based on object-based image analysis methods with the help of spectral indices. Image objects generated through segmentation were initially classified using SVM, which was followed by further classification using rule-sets based on expert knowledge.

The SVM classification was aimed at categorizing objects as either built-up or non-built-up or water based on three spectral indices: NDVI, VrNIR-BI, and NDWI. The initial results were assessed by overlay with high-resolution satellite imagery in Google Earth Pro. Firstly, it was noticed that some objects had been classified as built-up even though they were not. A check in the eCogniton made it clear that these areas in question had high VrNIR-BI and also low NDVI. This was primarily due to the absence of or low vegetation. Secondly, it was noticed that the VrNIR-BI and the NDVI of image objects mirrored each other hence VrNIR-BI was deemed a redundant feature for the algorithm.

The replacement of the VrNIR-BI with the NDBI and addition of DBSI refined the classification process. Although some non-built-up lands were still classified as built-up, it was way easier to assign them to their right classes using rules based on the value of the DBSI and NDVI. This suggests that the right combination of multiple spectral indices improves a classification process. Furthermore, the DBSI proved to be an important index to consider as an addition to the NDBI and perhaps any built-up index when extracting built-up areas in locations with dry climates as seen in Rasul et al. (2018). DBSI becomes indispensable for terrains of this nature where bare soil patches are mixed up with built-up patches in the same space.

The object-based approach provided additional leverage of using other image object features for the classification in the rule-sets. Features like the relationship of objects to neighbor objects, area, and location within a defined region were used in the eCognition environment to assign classes based on expert knowledge. This was especially useful when specific objects had to be assigned a class based on not only their spectral properties. Hence using these non-spectral features provided a means of narrowing the application of the rules to specific objects. An example is a case where a group of built-up patches identified to be sparsely vegetated lands was clustered at a portion of the image scene. By creating a virtual region that bounded these objects in eCognition, it was easy to assign them their right class without affecting the classifications of other objects with similar NDBI and NDVI values. This shows an advantage the object-based image analysis has over the pixel based. Furthermore, this method allows for some handy generalization operations: small objects in terms of their area that were completely bounded by objects of a different class were assigned the class of their bounding objects using rules following Tobler's first law of Geography (Hay et al.,2003). Although generating these rules for classification based on these object features were laborious, they were useful and enhanced the classification results.

Presence or absence of vegetation is captured well by a majority of spectral indices. Although the goal of the classification is to find (sparsely) vegetated areas there is a tendency of misclassification. Hence, an urban area with a good distribution of trees may have a low built-up index and may be classified as a low-density urban density area. While this classification may be correct in some cases, there is a tendency of misclassifying physically compact and dense areas with enough trees. Furthermore, the potential of this effect differs seasonally. Comparing the two cities to cities in Europe, a dissimilarity is noted in their urban landscape. The central parts of the Ghanaian cities have a good vegetation presence making it low-density compared to European cities, which have little to no vegetation in the

central parts and greener in the outskirts. Some land cover changes like the transition of vegetated areas to urban or sparsely vegetated areas were common to both study areas. Despite being common, these changes took a different pattern for both areas. In Accra, it is noticed that the gaps between urban patches by way of vegetated or sparsely vegetated lands gradually became urban. This supports the claim of Stow et al. (2016) which indicated that newly built-up area between 2000 and 2010 sprung up at the fringes of Accra. In effect, the once separate metropolises (Accra and Kumasi) are becoming close to each other to form one big urban agglomeration. Furthermore, small water bodies in parts of Accra gradually shrunk with some completely ending up as vegetated bare soils. This may be the results of anthropogenic activities around these water bodies for agricultural purposes or real estate. Accra in recent years has seen a boom in the real estate development with many developers building detached houses in the outskirts.

On the other hand, the sparsely vegetated patches around Kumasi expanded uniformly just as the urban areas expanded. Therefore, as the immediate sparsely vegetated patches became built-up ones, neighbor vegetated patches turned to sparsely vegetated patches. This is indicative of the nature of land use change in the area. Kumasi is situated in the Semi-Deciduous Rain forest ecological zone (Issaka et al., 2012) and the transformation of vegetated patches to sparsely vegetated is a sign of expanding built-up patches. Abass et al. (2018) are of the opinion that housing, road infrastructure, and industrial developments are reasons for the loss of vegetated cover. The clearance of the densely vegetated areas also paves the way for agricultural activities like grazing, small scale farms and economic ventures like charcoal production from fallen trees. Based on the assertions of Stow et al. (2016) and Acheampong et al., (2016) and Abass et al. (2018) these patches have a high probability to become built-up areas in future.

4.2 Urban processes and sprawl

While there may not be any widely accepted standard labels for urban processes, defining them based on land cover change experienced in the same area is a common process. A quintessential case is where spaces will be tagged as going through a process of urbanization based on the classical dichotomous (urban-rural) land cover classification as described by Inostroza et al. (2019). This suggests that the identifiable processes are limited by the depth of the land cover classification. With a good number of land cover classes, there is a chance of identifying different urban processes on finer scales. In this research, the definition of the urban processes reported is underpinned by the land cover changes that patches went through under the period of review.

Two main urban processes were identified namely densification and urbanization with each being later qualified into two types based on time of occurrence (Table 3). These processes are influenced by a wide range of dimensions such as historical city architecture, population growth, neighborhood segregations, etc. Given the processes that were named in the study areas, a few drivers were identified. These drivers are highlighted in the subsequent paragraphs which discuss the urban processes of the study areas.

The high-density urban core patches in Accra are mostly places where early settlers dwelled in the city for fishing and farming purposes like the Teshie township. Some of these areas are also iconic areas as they were places first European traders settled around the 16th century. Towns like James Town and Ussher Town are some places which have European influence. The other parts of high-density urban core patches are places that were developed in the post-independence era like Ashiaman and Tema New Town. The low-density urban core in Accra mostly covers the Accra central area and the Tema township. The expansion of Accra has been influenced by the migration of citizens from other parts of the country for economic gains and education. This process was triggered by the decision by the British government to make it the administrative capital of Ghana then known as Gold Coast (Owusu, 2013). Therefore, as the infrastructural development associated with capitals flourished, the number of inhabitants in Accra grew and different settlements sprung up. For instance, the entire

metropolis of Tema was built purposely to be a residential area for the heavy industries and the port built there. The University of Ghana and other tertiary educational institutions in Accra has played a fair role in attracting migrants to the city. Aside from migration, the natural increase in population has also been a driver of the urban processes (Owusu,2013).

While these events and key features of the area brought the people who facilitated urban expansion, the resulting urban processes were also influenced by in situ infrastructure, specifically roads. Referring to the urban process map (Figure 12), it is noticed that the urban densification in Accra occurred predominantly to the west with a few in the east and the north. This is no coincidence as it seems to follow the locations of the major roads (Figure 5) that connects the central part of Accra to the other parts. These roads also connect the Greater Accra region to other regions in the country. Mobility is one of the many if not the main reason for this pattern of development. These settlements are mostly dormitory towns as most people commute to the central part of Accra for work or school. This is because of the relatively cheap cost of housing and land compared to the central parts of Accra. From figure 2 the urbanized areas (both early and late) are arguably places that absorb the overspill of the densified areas as suggested by (Owusu,2013). Per the statistics from the Ghana Statistical Services (GSS) about half (2.4 million) the total population of Accra and Tema live in the districts which cover these areas of urbanization and densification.

For Kumasi, the high-density urban areas covered places like Tafo, Asokwa, and Aboabo. These areas are mostly in central Kumasi's iconic ring road (Figure 6) and its fringes. The low-density urban areas covered other parts of central Kumasi like Menhyia which serves as the cultural capital, Suame, and Amakom which are mainly commercial and residential areas. Being the second largest city in Ghana, Kumasi has received its fair share of migrants who hail from different parts of the country. The city is known for its commercial activities as it can boast of some of the biggest markets in Ghana. The geographical location has made it important for trading between southern and northern Ghana. Just like Accra, Kumasi was also a place of interest for the British colonial government which implemented a garden city model (Adjei, 2014). Unfortunately, the urban processes and the demand for space within the city gave away the garden spaces for concrete and asphalt. For instance, a once-popular park the Para Gardens has currently been replaced by the Sofoline interchange, a major road infrastructure (Adjei, 2014). Referring to figure 12, the urban processes (densification and urbanization) occurred evenly in all directions. Once again this comes as no coincidence. Looking at figure 6 gives the idea that these processes occurred around the major traffic arteries that connect central Kumasi to other major towns in the region. In this case, mobility and access to the central business district bounded by the ring road could be driving factors of this development pattern. The expansion, especially the later urbanized areas are mostly outside the current urban extent of Kumasi. These settlements are mostly dormitory areas.

It is evident that the major roads in both study areas have influenced where the urban processes occur. Hence, the development in both areas is in the form of a ribbon or strip development (Oduro et al., 2014). Referring to table 4, the rate of creating new urban areas or sprawl was higher in the first period for Accra compared to the second period. Also, the densification rate for Accra was less in the first period compared to the second. The urbanization rate outweighed the densification rate in the first period. In the second period, the densification rate almost matched the urbanization rate. Therefore, the area of land that became sprawled in the last period was nearly the same area of built-up patches which were densified in the same period. In the case of Kumasi, the rate for urbanization and densification were almost the same for both periods. Hence for the sprawl rates were nearly the same in both periods. Sprawling in Kumasi also outweighed densification (Table 4).

In general, the entire urban space of Accra and Kumasi increased by 91.6% and 140% respectively for the whole study period (Table 2). These rates exceed the population growth rates for both cities. For the entire period, the population of Accra and Kumasi increased by 47.8% and 65.4% respectively per

information from GSS. This implies the cities are expanding at a rate faster than that of population. The GSS reports of great housing deficits in these two cities which exceeds more than half of their respective housing stocks (Ghana Statistical Services, 2014d). Matching the rate of urban expansion, the population growth and the housing deficit report shows an effect of sprawl. The cities are sprawling mainly for residential purposes but cannot still cater to the housing needs of the people, hence implying an injudicious use of land (Karakayaci, 2016).

4.3 Land surface temperature and heat islands

The land surface temperature generated from thermal remote sensing is a widely acceptable parameter for assessing UHI. In addition, given that temperature is a continuous variable, estimating surface temperatures from several discrete measurements will not be apt in terms of the resolution to assess UHI.

The relationship between the land cover and temperature reveals how surface materials influence temperatures. Most important of all is vegetation. Vegetation reduces temperatures through evapotranspiration and by casting shades (US-EPA, 2008) commonly known as a cooling effect. Therefore, the absence of vegetation (cooling effect) on the bare soil patches makes them warmer. This makes their LST similar to artificial (built-up) surfaces. By this reasoning also, the temperatures of the built-up areas and the relatively low temperatures of vegetated patches are justified.

Following the definition of UHI by the US-EPA (2008) and the definition of rural and urban with respect to this research, the intensity of UHI was assessed by computing the SUHII (Table 7). The intensity values are indicative of the difference between temperatures of built-up and non-built-up land cover types. Although this means of assessment is informative as it provides urban and rural temperature differences, it does not reveal where in space are the hottest regions. To overcome this limitation, the SUHIM is also employed as an additional mean of assessment. SUHIM in addition to identifying the hottest region in space allows for the determination of the mean temperature difference between the hottest region and the other parts (Table 8).

Although the figures in table 7 indicate that the urban areas are warmer than the rural, it was expected that these values would have been higher. This expectation was unmet because the mean surface temperature of the rural areas was greatly influenced by the high temperatures of bare soils and sparsely vegetated patches. The SUHII for Accra in 2017 was significantly greater than the 2002 and 2011. The conversion of bare soils and sparsely vegetated soils to urban patches is a reason for this as it reduced the mean temperature of rural areas. In the case of Kumasi, the value for 2002 in terms of SUHII is greater than that of 2017. This does not necessarily mean the urban area became less warm over time. Considering the land cover changes in Kumasi, the rural area was largely made up of vegetated patches which have a relatively low surface temperature. This influenced the mean surface temperature of the rural area and subsequently resulted in higher SUHII. By 2017, most of the vegetated patches had become sparsely vegetated and as a result, had warmer surface temperatures. This change in cover influenced the mean surface temperature of the rural areas. As a result, the difference in temperature between the built-up area and non-built-up area diminished and gave a low SUHII for 2017. For 2010, in Kumasi, the influence of extremely warm days on the SUHII is noticeable.

Moving on to the SUHIM, the influence of land cover types is noticed even though the assessment is not entirely based on the land cover type. The values in table 8 for Accra create the impression of a reducing magnitude. Again, this may not necessarily be the case. Considering figure 14, it is noticed that there have been shifts in the location of the hottest region (> mean+std) along with the reduction of its area in the three maps for Accra. Matching these maps to the land cover maps makes it clear that most of the sparsely vegetated and the bare soils constituted the hottest regions together with built-up patches. As the sparsely vegetated and bare soil patches became built-up, the hottest region shifted, shrank and localized at built-up areas (especially high-urban density). In the case of Kumasi, the hottest region matched the built-up extent fairly. This is because of the nature of the land cover distribution. Even though by the 2010 and 2017 significant vegetated patches had been converted to sparsely

vegetated, they did not form part of the hottest region like it was in the case of Accra. This is primarily because of their temperatures were below the threshold. Furthermore, the difference in the ecological zones for both cities could be a factor. The nature of the ecological zone for Kumasi guarantees healthier vegetation compared to the coastal savannah which is for Accra.

While the SUHIM provides a difference in temperature between the hottest region and the rest of the study area, the resulting maps cannot be relied on to identify built-up areas. Especially for landscapes with a presence of bare soil and sparsely vegetated patches in dry climates.

Comparing SUHII values for Accra and Kumasi to values in Berlin in Li et al. (2018), the Ghanaian cities had lower SUHII values. The SUHII for Berlin ranged from 3.91 °C to 6.55 °C. In comparing the SUHIM of the Ghanaian cities to European cities studied by Ward et al. (2016), it is noticed that the values of the Ghanaian cities are higher. The study of Ward et al. (2016) focused on assessing SUHIM during the heat waves in the summer of 2016. The SUHIM of Accra and Kumasi were greater than all the European cities. Although the SUHIM of these European cities were exacerbated by the heat waves, they were still lower than the SUHIM of normal days in Ghana. The difference in the urban configurations and climatic zones are possible reasons for these differences.

Considering the SUHII for both study areas, urban dwellers potentially face the effects of UHI like impaired air quality and discomfort especially in events of heat waves. If sparsely vegetated and bare soil patches progress to become built-up as witnessed, the SUHII in both study areas is likely to increase. Focusing on the hottest regions (SUHIM), it is evident that land cover changes and the urban processes, especially densification, influence its location. In the case of Accra, the hottest region for 2017 lied outside the central parts where most commercial and industrial activities take place. It covered sections that are mostly residential. Depending on the mobility patterns of citizens and their activities in time and space, some people may be more exposed to the dangers of warm temperatures. For instance, the elderly, housewives and lactating mothers and infants below school-going age who spend most of their time at home are more exposed and stand a high chance of being diagnosed with heat-related illnesses. In the case of Kumasi, the hottest region follows is covers almost the entire urban agglomeration which makes those who work and live there more vulnerable. In both cities, people who are well-to-do can afford the AC to reduce the discomfort leaving the poor more vulnerable.

Conclusions

Increasing population results in urbanization. With urbanization comes undesired phenomena namely sprawl and UHI. These undesired phenomena pose a threat to the health and the comfort of urban dwellers. These further undermine the liveability of urban places. The volume of research done to cover these phenomena is justified when their impacts are considered. It is important that sprawl and UHI be studied in all parts of the world to suggest bespoke measures. This research adds up to the effort to bridge the lacuna in tropical UHI studies and also identify how urban processes influence UHI in tropical cities.

This research focused on identifying sprawl pattern and extent in two major Ghanaian cities (Accra and Kumasi) and how they compared over the period of 2002 to 2017 using remote sensing imagery. UHIs in the cities were also detected and sprawl influences on UHIs in these cities over the study period were investigated.

The research employed remotely sensed images from Landsat 7 and 8 missions for mapping land cover of the study areas to detect sprawl. Three images were collected for each study area covering the years 2002, 2010(Kumasi), 2011(Accra) and 2017. The Land Surface Temperature (LST) relevant for detecting the UHI was also generated using the thermal band of the images. The analysis involved mainly GIS operations, Object-Based Image Analysis (OBIA) and thermal remote sensing. GIS operations covered buffer analysis, zonal statistics and map algebra. OBIA involved image segmentation and classification using support vector machine and knowledge-based approach. For thermal remote sensing, the single channel algorithm for estimating LST was used.

The land cover changes suggest a significant area of non-built-up lands especially bare soils and sparsely vegetated lands became built-up in Accra. In Kumasi, a similar trend was noticed. Interestingly, a large area of vegetated lands became sparsely vegetated lands which were influenced by the expansion of the built-up area. Furthermore, the urban processes revealed that urbanization and densification were the main urban processes. Urbanization in Accra was at a faster pace compared to densification in the first period but both processes had almost equal rates in the second period. On the other hand, the urbanization and the densification processes in Kumasi had fairly the same rates for both periods. The sprawl was identified to occur at the outskirts of the urban cores and followed a ribbon development pattern. The urban expansion rates for both cities outweigh their respective population growth rate. Migration, the natural increase of population, mobility, cost of housing, and low land prices are some drivers identified to influence the patterns of sprawl.

UHI analysis using the SUHII and SUHIM gave the opportunity to assess the influence of land cover and the urban processes on UHI. The SUHII and SUHIM values indicate the presence of UHI in both cities. In the case of SUHII, it was noticed that non-built-up cover classes like bare soils and sparsely vegetated had also high temperature, which caused low SUHII value. These cover types are likely to increase the overall urban temperature if they are abundant in urban spaces even though they are not built-up. SUHIM, on the other hand, revealed the hottest regions in the study area. In Accra, a shift and a decrease in size were noticed with regards to the hottest region. These were primarily influenced by land cover changes from bare soils to built-up lands and densification. In Kumasi, the hottest region expanded and matched the shape of the urban expansion with no significant shifts. The SUHIM values were relatively higher compared to values for European cities during the heat wave of 2016. Although urban configurations and climatic conditions may be the reason for the differences, this shows how alarming and dangerous UHI could be in tropical cities. The influence of extremely hot days on UHI in tropical cities is highlighted by the SUHIM and SUHII for 2010 in Kumasi.

In conclusion, Accra and Kumasi expanded significantly over the 15-year period with urbanization being the lead urban process followed by densification. The nature of sprawl is similar for both study areas. Given the nature of expansion, Accra and Tema are likely to form a single urban agglomeration while Kumasi will have an urban transition zone with adjoining municipalities. The UHI present in

both cities are greatly influenced by the land cover types and urban processes. The results show that the land cover changes affected the hottest regions (SUHIM) and intensities (SUHII). If the urban expansion continues, the SUHII is likely to appreciate and will be worsened on extremely warm days.

Kokkuvõte

Magistritöö linnalistunud ühiskonna geoinformaatikas: Valglinnastumise dünaamika ja linna kuumasaared (UHI) Ghanas

Sedamööda, kuidas inimeste arv suureneb, muutub suuremaks ka vajadus majutuse ja muu vajaliku taristu järele, mis teeb elu mugavamaks. Selle tagajärjel linnastuvad ka maapiirkonnad, et seda vajadust rahuldada (Bharath et al., 2018). See võib tekitada valglinnastumist, mida iseloomustab linnaliste alade kontrollimatu ja planeerimatu väljapoole laienemine (Karakayaci, 2016; Antrop 2018). Veel üks maapiirkondade linnaliseks muutumise otsene tagajärg on looduslike maa-alade asendamine vett mitte läbilaskvate ja kuumust koguvate pindadega nagu betoon ja asfalt (Madanian et al., 2018). Lisaks loodusliku maastiku muutumisele muudab see maapinna katte vahetumine ka maapinna ja atmosfääri vahelist energiavahetust, mis omakorda mõjutab mikrokliima muutujaid nagu temperatuur ja maapinnalähedane tuul (Madanian et al., 2018). Selline mõju mikrokliima muutujatele nagu temperatuurile toob kaasa nähtuse, mida nimetatakse linna kuumasaarteks (UHI) (Voogt ja Oke, 2002). Käesolevas uuringus klassifitseeritakse uuringuala madala tihedusega hoonestusega osa maapiirkonnaks ja suure tihedusega hoonestusega osa linnaliseks piirkonnaks.

UHI omab mõju ka inimeste tervisele, sest on täheldatud, et see soodustab õhukvaliteedi langust ja vähendab veekvaliteeti (US-EPA, 2008). Santamouris et al. (2005) märgivad, et selle nähtuse mõju ei piirdu ainult tervisega, vaid hõlmab ka majanduslikku mõju. WMO ja WHO (2015) märgivad, et troopilistes piirkondades, kus kuumalained polnud varem probleem, on need nüüd murettekitavad, kuna seal on tekkinud linnastumine ja sellega kaasnevad UHI-d. Kahtlemata vähendab UHI mõju linnalisele alale selle elatavust (Sidiqui et al., 2016). Õhukvaliteet ja tervis on koha elatavuse peamised mõõdikud (Kennedy ja Buys, 2010). Seepärast annab nende mõõdikute halvenemine mis tahes piirkonnas põhjust uurida nähtuse olemust, et pakkuda välja sobivaid leevendusmeetmeid (Sidiqui et al., 2016).

Käesolev uuring keskendus sellele, et tuvastada märkimisväärsed valglinnastuvad alad ja nende ulatus kahes suuremas Ghana linnas (Accra ja Kumasi) perioodil 2002 kuni 2017, kasutades kaugseiret. Samuti tuvastati linnades UHI-d ja valglinnastumise mõju UHI-de kasvule neis linnades uurimisperioodi jooksul.

Uuringus kasutati kaugseire andmeid NASA Landsat 7 ja 8 missioonidest, et kaardistada uuringuala maakate, leidmaks valglinnastumise alad. Iga uuringuala kohta koguti kolm kujutist, mis hõlmasid aastaid 2002, 2010 (Kumasi), 2011 (Accra) ja 2017. UHI tuvastamiseks vajalikud maapinna temperatuuri (LST) andmed genereeriti samuti kujutiste termoandmeid kasutades.

Analüüs hõlmas peamiselt GIS operatsioone, objektipõhist kujutiseanalüüsi (OBIA) ja termilist kaugseiret. GIS operatsioonid hõlmasid puhvrianalüüsi, tsoonistatistikat ja kaardialgebrat. OBIA hõlmas kujutiste segmenteerimist ja klassifitseerimist, kasutades tugivektorite masinat ja teadmispõhist lähenemist. Termilise kaugseire jaoks kasutati ühekanalilist algoritmi, millega hinnati LST andmeid.

Maakate jagati kuude klassi, nimelt kõrge linnatihedus, madal linnatihedus, paljas pinnas, hõre taimestik, taimestik ja vesi. Tulemused näitavad, et uuringuperioodi jooksul muutusid mõlemas uuringualas paljad pinnased ja hõreda taimestikuga kohad linnalisteks aladeks. Kumasis leiti, et taimestikuga alad muutusid aja jooksul hõreda taimestikuga aladeks. Oli huvitav tuvastada mõlemas uuringualas toimuvad linnalised protsessid. Protsesside tuvastamise aluseks olid maakatte muutused 2002. aastal, mis võeti baasaastaks. Samaks jäänud linnalised pinnakatted loeti tuumikuteks (kõrge linnatihedus ja madal linnatihedus). Tihenemine ja linnastumine olid kaks peamist tuvastatud protsessi. Sõltuvalt nende kahe protsessi toimumise ajast märgiti nii linnastumine kui tihenemine varajaseks või hiliseks. Varajane tähendas protsesse, mis toimusid uuringuperioodi keskel (2010/2011)

ja hiline tähendas neid, mis toimusid aastaks 2017. Varakult linnastunud alad, mis hiljem muutusid tihedalt hoonestatuks, loeti varajaseks linnastumiseks koos hilise tihenemisega.

Leiti, et andmetest genereeritud maapinna temperatuur vastas maapinna katte tüübile. Kõrge linnatihedusega aladel olid kõrgemad temperatuurid kui madala linnatihedusega aladel. Paljad pinnased ja hõreda taimestikuga alad ei olnud küll hoonestatud, kuid seal olid pinnatemperatuuri osas hoonestatud aladele sarnased kuumustingimused. Kasutati kaht meetodit kuumasaarte hindamiseks, nimelt linnaliste kuumasaarte intensiivsust (Surface Urban Heat Island Intensities – SUHII) ja linnaliste kuumasaarte pinna magnituudi (Surface Urban Heat Island Magnitude – SUHIM). SUHII näitas, millist mõju avaldasid maapinna katte tüübid hoonestatud ja hoonestamata alade vahelisele temperatuuride erinevusele. SUHIM aga näitas uuringuala kõige kuumemaid piirkondi vastavalt kättesaadavale statistikale.

Sisuliselt oli maakasutuse muutus hoonestamata aladest hoonestatud aladeks mõlemas piirkonnas märkimisväärne. Kumasi alad, kus taimestikust on saanud hõre taimestik, muutuvad tõenäoliselt varsti linnalisteks. Peamiseks linnaliseks protsessiks oli linnastumine, millele mõlemas piirkonnas järgnes kohe tihenemine. Samuti pandi tähele, et mõned maapinna katte tüübid võivad anda panuse kuumasaarte tekkimisse, kui neid on linnalises alas palju. Ja lõpuks tuvastati Kumasi puhul äärmiselt soojade päevade halvendav mõju SUHII ja SUHIM-i tulemustele.

Acknowledgment

Heartfelt thanks to my supervisors Dr. Valentina Sagris and Iuliia Burdun for providing guidance and support in executing this research. I am grateful for their contributions. Special thanks to Dr. Dirk Tiede for refining my ideas and the OBIA lab at Z_GIS-University of Salzburg for their insightful consultations. I am grateful for the immense support given to me by Trimble. The eCognition® developer version license provided by Trimble was instrumental for the success of this research and I appreciate their support. Special thanks to my friends at CERGIS for helping me out with data acquisition. Finally, thank you to all friends and family in Ghana, Estonia, USA and Austria for their continuous support and encouragements.

References

Abass K., Adanu S.K., Agyemang S., 2018. Peri-urbanization and Loss of Arable Land in Kumasi Metropolis in Three Decades: Evidence from Remote Sensing Image Analysis, *Land Use Policy*, 72, 470–479.

Acheampong, R. A., Agyemang, F. S. K., Abdul-Fatawu, M. 2016. Quantifying the Spatio-temporal Patterns of Settlement Growth in a Metropolitan Region of Ghana. *GeoJournal*, 82, 823-840.

Adjei M. C., 2014. Is Kumasi still a garden city? land use analysis between 1980 and 2010. *Journal of Environment and Ecology* 5 (2), 89–107.

Akbari H., 2005. Energy Saving Potentials and Air Quality Benefits of Urban Heat Island Mitigation, Heat Island Group, Lawrence Berkeley National Laboratory.

Al-doski J., Mansrol S. B., Shafri H. Z. M., 2012. Image Classification in Remote Sensing, *Journal of Environment and Earth Science*, 3(10), 141-148.

Amer K., Parham P., Behnaz B., 2017. Land Use Analysis on Land Surface Temperature in Urban Areas Using a Geographically Weighted Regression and Landsat 8 Imagery, a Case Study: Tehran, Iran. *The International Archives of the Photogrammetry, Remote Sensing and Spatial Information Sciences*, 42, 117-122.

Amorim M. C. de C. T., Dubreuil V., 2017, Intensity of Urban Heat Islands in Tropical and Temperate Climates, *Climate*, 5(4), 1-13.

Angel, S., Parent, J., & Civco, D., 2007. Urban Sprawl Metrics: An Analysis of Global Urban Expansion Using GIS. *Proceedings of ASPRS 2007 Annual Conference*, Tampa, Florida May 7–11.

Antrop M., 2018. Landscape Ecology in an Urbanising Society, Lecture Notes, University of Tartu, Estonia.

Ardayfio-Schandorf E., Yankson P. W. K., Bertrand M., 2012. *The Mobile City of Accra, Urban Families, Housing and Residential Practices*, CORDERDIA, Dakar-Senegal.

Asante, A.F., Amuakwa-Mensah, F., 2014. Climate Change and Variability in Ghana: Stocktaking, *Climate*, 3, 78-99.

Bakker, W. H., Janssen, L. L. F., Reeves, C. V., Gorte, G. H. B., Pohl, C., Weir, M. J. C., Horn, J. A., Prakash, A. & Woldai, T. 2001. Principles of Remote Sensing- An introductory textbook, Enschede, The Netherlands, The International Institute for Aerospace Survey and Earth Sciences.

Barsi J. A., Barker J. L., Schott J. R., 2013. An Atmospheric Correction Parameter Calculator for a single thermal band earth-sensing instrument, *IGARSS 2003. 2003 IEEE International Geoscience and Remote Sensing Symposium. Proceedings (IEEE Cat. No.03CH37477)*, Toulouse,5,3014-3016.

Baatz, M., Schape, A., 2000, Multiresolution Segmentation: An Optimization Approach for High-Quality Multi-Scale Image Segmentation. In: Strobl, J., Blaschke, T. and Griesbner, G., (eds)., Angewandte Geographische Informations-Verarbeitung, XII, Wichmann Verlag, Karlsruhe, Germany, 12-23.

Bharath H.A., Chandan M.C., Vinay S., Ramachandra T.V.,2018, Modelling Urban Dynamics in Rapidly Urbanising Indian Cities, *The Egyptian Journal of Remote Sensing and Space Science*,21(3), 201-210.

Bhargava A., Lakmini S., Bhargava S., 2017. Urban Heat Island Effect: Its Relevance in Urban Planning, *Journal of Biodiversity & Endangered Species*,5(2), 1-4.

Bhat P. A., Ul Shafiq, M., Mir, A. A., Ahmed, P. 2017. Urban sprawl and its impact on land use/land cover dynamics of Dehradun City, India. *International Journal of Sustainable Built Environment*, 6, 513–521.

Bhatta B., Saraswati S., Bandyopadhyay D., 2010. Urban Sprawl Measurement from Remote Sensing Data, *Applied Geography*, 30, 731-740.

Blaschke T., Strobl J. 2001, What's wrong with pixels? Some recent developments interfacing remote sensing and GIS. *GIS – Zeitschrift für Geoinformationssysteme*, 14, 12 - 17.

Bouhennache R., Bouden T., Abdmalik A. T., 2014. Change Detection in Urban Land Cover Using Landsat Images Satellites, A Case Study in Algiers Town, *The 10th International Conference on Signal Image Technology & Internet Based Systems*, 622-628.

Cobbinah P. B. and Aboagye H.N, 2016. A Ghanaian twist to urban sprawl, *Land Use Policy*, 61, 231-241.

Cobbinah P., Niminga-Beka R., 2017. Urbanisation in Ghana: Residential land use under siege in Kumasi Central. *Cities*. 60. 388-401.

Codjoe N. A. S., Nabie A. V., 2014, Climate Change and Cerebrospinal Meningitis in the Ghanaian Meningitis Belt, *International Journal of Environmental Research and Public Health*, 11, 6923-6939.

Cristóbal, J., Jiménez-Muñoz, J. C., Prakash, A., Mattar, C., Skokovic, D., & Sobrino, J. A., 2018. An Improved Single-Channel Method to Retrieve Land Surface Temperature from the Landsat-8 Thermal Band, *Remote Sensing*, 10(431), 1-14.

Estoque R. and Murayama Y., 2015. Classification and Change Detection of Built-Up Lands from Landsat-7 ETM+ and Landsat-8 OLI/TIRS Imageries: A Comparative Assessment of Various Spectral Indices, *Ecological Indicators*, 56, 205–217.

Ewing R, 2008. "Characteristics, Causes, and Effects of Sprawl: A Literature Review", in Urban Ecology Eds J M Marzluff, E Shulenberger, W Endlicher, M Alberti, G Bradley, C Ryan, C ZumBrunnen, U Simon (Springer, New York), 519–535.

Filho, W.L, Icaza, L.E., Neht, A., Klavins, M., Morgan, E.A., 2018, Coping with the Impacts of Urban Heat Islands. A Literature Based Study on Understanding Urban Heat Vulnerability and the Need for Resilience in Cities in a Global Climate Change Context, Journal of Cleaner Production,171,1140-1149.

Freudenberg, N., Galea, S., Vlahov, D. 2005. Beyond Urban Penalty and Urban Sprawl: Back to Living Conditions as The Focus of Urban Health, *Journal of Community Health*, 30, 1-10.

Frumkin, H. 2002. Urban Sprawl and Public Health, *Public Health Reports*, 117, 201-217.

Galster, G., Hanson, R., Wolman, H., Coleman, S., & Freihage, J., Rathcliffe, M. R., 2001. Wrestling Sprawl to the Ground: Defining and Measuring an Elusive Concept, *Housing Policy Debate*, 12(4), 681–717.

Gandhi, S. R., Sharma, S. A., Vyas, A. 2016. Quantifying Urban Sprawl for Rajkot City using Geospatial Technology, *International Journal of Built Environment and Sustainability*, 3, 86-92.

Ghana Statistical Services, 2014a, 2010 Population and Housing Census Report-Urbanization, Ghana Statistical Services, Accra.

Ghana Statistical Services, 2014b, 2010 Population and Housing Census District Analytical Report-Accra Metropolitan, Ghana Statistical Services, Accra.

Ghana Statistical Services, 2014c, 2010 Population and Housing Census District Analytical Report-Kumasi Metropolitan, Ghana Statistical Services, Accra.

Ghana Statistical Services, 2014d, Housing in Ghana, Ghana Statistical Services, Accra.

Irwin, E. G., Bockstael, N. E. 2007. The Evolution of Urban Sprawl: Evidence of Spatial Heterogeneity and Increasing Land Fragmentation, *Proceedings of the National Academy of Sciences of the United States of America*, 104, 20672–20677.

Giridharan, R. and Emmanuel, R., 2018. The impact of urban compactness, comfort strategies and energy consumption on tropical urban heat island intensity: a review. *Sustainable Cities and Society*, 40, 677-687.

Hay G. J, Blaschke T., Marceau D. J., Bouchard A. 2003. A Comparison of Three Image-object Methods for the Multiscale Analysis of Landscape Structure, *ISPRS Journal of Photogrammetry and Remote Sensing*, 57(5–6), 327-345.

Inostroza L., Hamstead Z., Spyra M., Qureshi S., 2019. Beyond Urban-Rural Dichotomies: Measuring Urbanisation Degrees in Central European Landscapes Using the Technomass as an Explicit Indicator, *Ecological Indicators*,96(1).

Issaka, R., Buri, M., Tobita, S., Nakamura, S., Owusu-Adjei, E. 2012. Indigenous Fertilizing Materials to Enhance Soil Productivity in Ghana. In: WHALEN, J. (ed.) Soil Fertility Improvement and Integrated Nutrient Management-A Global Perspective.

Jat M.K., Garg P.K., Khare D., 2007. Monitoring and Modelling of Urban Sprawl Using Remote Sensing and GIS Techniques, *International Journal of Applied Earth Observation and Geoinformation*,10, 26-43.

Jiménez-Muñoz, J. C., Cristóbal, J., Sobrino, J. A., Sòria, G., Ninyerola, M. & Pons, X. 2009. Revision of the Single-Channel Algorithm for Land Surface Temperature Retrieval from Landsat Thermal-Infrared Data, *IEEE Transactions on Geoscience and Remote Sensing*, 47, 11, 339-349.

Kankam-Yeboah K., Amisigo B., Obuobi E., 2010. Climate Change Impacts on Water Resources in Ghana., The Pan-African Workshop on "Decision-Making Support for Coastal Zone Management, Water Resources and Climate Change in Africa", UNESCO, Cotonou, Benin.

Karakayaci Z., 2016. The Concept of Urban Sprawl and its Causes, *the Journal of International Social Research*, 45(9), 815-818.

Kennedy R. J., & Buys L.,2010. Dimensions of Liveability: a Tool for Sustainable Cities. in *Proceedings of SB10mad Sustainable Building Conference*, Madrid.

Kimuku C.W., Ngigi M., 2017. Study of Urban Heat Island Trends to Aid in Urban Planning in Nakuru County-Kenya, *Journal of Geographic Information System*, 9, 309-325.

Li H., Zhou Y., Li X., Wang X., Wu S., Sodoudi S., 2018. A New Method to Quantify Surface Urban Heat Island Intensity, *Science of the Total Environment*, 624, 262–272.

Li J, Wang X., Wang X., Ma W., Zhang H., 2009. Monitoring Patterns of Urban Heat Islands of the Fast-growing Shanghai Metropolis, China: Using Time-series of Landsat TM/EMT+ Data, *International Journal of Applied Earth Observation and Geoinformation*, 12, 127-138.

Li Y., Zhang H., Kainz W., 2012. Remote Sensing Evaluation of Urban Heat Islands and its Spatial Pattern of the Shangai Metropolitan Area, China, *Ecological Complexity*, 6, 413-420.

Loveland T., Crawford J. C., Masek J., Wulder M., 2018. An Overview of USGS-NASA Landsat Science Team Activities During 2018, *The Earth Observer*, 30(5), 19-26.

López-Serrano, P. M., Corral-Rivas, J. J., Díaz-Varela, R. A., Álvarez-González, J. G., López-Sánchez, C. A. 2016. Evaluation of Radiometric and Atmospheric Correction Algorithms for Aboveground Forest Biomass Estimation Using Landsat 5 TM Data. *Remote Sensing*, 8,1-19.

Madaniana M., Soffianiana A. R., Koupaia S.S., Pourmanaf S., 2018. The Study of Thermal Pattern Changes Using Landsat-derived Land Surface Temperature in the Central Part of Isfahan Province, *Sustainable Cities and Society*, 39, 650-661.

Manu, A., Twumasi, Y. A., Coleman, T. L. 2006. Is It the Result of Global Warming or Urbanization? The Rise in Air Temperature in Two Cities in Ghana. *5th FIG Regional Conference: Promoting Land Administration and Good Governance*. Accra, Ghana: FIG,1-14.

Matthew, M. W., Adler-Golden, S. M., Berk, A., Felde, G., Anderson, G. P., Gorodetsky, D., Paswaters, S. & Shippert, M. Atmospheric Correction of Spectral Imagery: Evaluation of the FLAASH Algorithm with AVIRIS Data. *Applied Imagery Pattern Recognition Workshop*, 2002 Washington, DC, USA. Spectral Sciences, Inc., 157-163.

McGranahan G., Satterthwaite D., 2014. Urbanization Concepts and Trends. International Institute for Environment and Development, Available at www.jstor.org/stable/resrep01297.

Meng Q., Zhang L., Sun Z., Meng F., Wang L., 2018. Characterizing Spatial and Temporal Trends of Surface Urban Heat Island Effect in An Urban Main Built-Up Area: A 12-Year Case Study in Beijing, China, *Remote Sensing of Environment*, 204, 826–837.

Mensah, C., Atayi, J., T. Kabo-bah, A., Švik, M., Acheampong, D., 2018, Assessing the Impacts of Urbanization on the Climate of Kumasi, *Preprints*.

Nabi, S., & Qader, S. 2009. Is Global Warming likely to cause an increased incidence of Malaria? *The Libyan journal of medicine*, 4(1), 18-22. doi:10.4176/090105

Oduro, C. Y., Ocloo, K., Peprah, C. 2014. Analyzing Growth Patterns of Greater Kumasi Metropolitan Area Using GIS and Multiple Regression Techniques. *Journal of Sustainable Development*, 7, 13-31.

Orenstein D. E., and Frenkel A., 2012. Methodology Matters: Measuring Urban Spatial Development Using Alternative Methods, Environment, and Planning B: *Planning and Design*, 41, 3-23.

Osei E.F., Balogun B., Africa C.G., 2015. Identifying and Quantifying Urban Sprawl in the Greater Accra Region of Ghana from 1985 to 2014, *International Journal of Science and Research (IJSR)*, 4(1).

Owusu G., 2013. Coping with Urban Sprawl: A Critical Discussion of the Urban Containment Strategy in a Developing Country City, Accra, Planum. *The Journal of Urban*ism, 26(1), 1-17.

Owusu-Ansah, J.K., O'Connor, K.B., 2010. Housing Demand in the Urban Fringe around Kumasi, Ghana. *Journal of Housing and Built Environment*. 25 (1), 1–17.

Rajagopalan P., Lim C.K., Jamei E. 2014. Urban Heat Island and Wind Flow Characteristics of a Tropical City, *Solar Energy*, 107, 159‑170.

Rasul A., Balzter H., Ibrahim G.R.F., Hameed H.M., Wheeler, J., Adamu B., Ibrahim, S., Najmaddin, P.M., 2018, Applying Built-Up and Bare-Soil Indices from Landsat 8 to Cities in Dry Climates. *Land*, 7, 81.

Rokni, K., Ahmad, A., Selamat, A. & Hazini, S. 2014. Water Feature Extraction and Change Detection Using Multitemporal Landsat Imagery, *Remote Sensing*, 6, 4173-4189.

Sagris V., Sepp M., 2017. Landsat 8 TIRS Data for Assessing Urban Heat Island Effect and its Impact on Human Health. *IEEE Geoscience and Remote Sensing Letters*, 14 (12), 1−5.

Santamouris M., Cartalis C., Synnefa A., Kolokotsa, 2014. On the Impact of Urban Heat Island and Global Warming on the Power Demand and Electricity Consumption of Buildings-A Review, *Energy and Buildings*, 98, 119-124.

Schwarz, N., Lautenbach S., Seppelt R., 2011. Exploring Indicators for Quantifying Surface Urban Heat Islands of European Cities with MODIS Land Surface Temperatures, *Remote Sensing of Environment*,115 (2012), 3175–3186.

Sidiqui P., Huete A., Devadas R., 2016. "Spatio-temporal mapping and monitoring of Urban Heat Island patterns over Sydney, Australia using MODIS and Landsat-8," *4th International Workshop on Earth Observation and Remote Sensing Applications (EORSA)*, Guangzhou.

Silva J.S., Silva R.M., Santos C. A. G., 2018. Spatiotemporal Impact of Land Use/Land Cover Changes on Urban Heat Islands: A case study of Paço do Lumiar, Brazil, *Building and Environment*,136, 279–292.

Stemn, E., Agyapong, E., 2014, Assessment of Urban Expansion in the Sekondi-Takoradi Metropolis of Ghana Using Remote-Sensing and GIS Approach, *International Journal of Science and Technology*, 3(8), 452-460.

Stow D. A., Weeks J. R., Shih H., Lloyd L., Johnson C. H., Tsai Y., Kerr A., Benza M., Mensah F., 2016. Inter-regional Pattern of Urbanization in Southern Ghana in the First Decade of the New Millennium, *Applied Geography*, 71, 32-43.

Sobrino, J. A. & Jiménez-Muñoz, J. C. 2010. A Single-Channel Algorithm for Land-Surface Temperature Retrieval from ASTER Data, *IEEE Geoscience, and Remote Sensing Letters*, 7(1), 176-179.

Sobrino, J. A., Jiménez-Muñoz, J. C. & Paolini, P. 2004. Land Surface Temperature Retrieval from LANDSAT TM 5, *Remote Sensing of Environment*, 90, 434-440.

Songsore J., 2009. The Urban Transition in Ghana: Urbanization, National Development, and Poverty Reduction, *IIED-UNFPA Research Meeting on Population and Urbanization Issue*s, London, UK, 1-79.

Stanturf J., Melvin L. Wareen J., Charnley S., Polasky S., Scott L., Armah F., Atuahehne N. Y, 2011. Ghana Climate Change Vulnerability and Adaptation Assessment, USAID.

Thomas H., T., Butters C., P., 2017. Thermal Equity, Public Health, and District Cooling in Hot Climate Cities, *Proceedings of the Institution of Civil Engineers-Municipal Engineer*, 171(3), 163-172.

U.S. Environmental Protection Agency. 2008. Reducing Urban Heat Islands: Compendium of Strategies. Draft. https://www.epa.gov/heat-islands/heat-island-compendium

USGS, 2016, Landsat—Earth Observation Satellites, USGS Factsheets.

USGS, n.d., How can I tell the difference between Landsat Collections data and Landsat data I have downloaded in the past?, Available at: https://www.usgs.gov/faqs/how-can-i-tell-difference-between-landsat-collections-data-and-landsat-data-i-have-downloaded, Accessed 26 May 2019.

van Der Hoeven F., Wandl A., 2018. Hotterdam: Mapping the social, morphological, and land-use dimensions of the Rotterdam urban heat island. *Urbani Izziv*, 29(1), 58-72.

van Ham M., Tammaru T., de Vuijst E., Zwiers M., 2016. Spatial Segregation and Socio-Economic Mobility in European Cities, *Discussion Paper Series*,1-21.

Vittek, M., Brink, A., Donnay, F., Simonetti, D., Desclée, B., 2014. Land Cover Change Monitoring Using Landsat MSS/TM Satellite Image Data Over West Africa between 1975 and 1990, *Remote Sensing*, 6, 658-676; doi:10.3390/rs6010658.

Voogt, J.A., Oke, T.R., 2003. Thermal Remote Sensing of Urban Climates. *Remote Sensing of Environment*. 86, 370–384.

Ward, K., Lauf S., Kleinschmit B., Endlicher W., 2016. Heat Waves and Urban Heat Islands in Europe: A review of Relevant Drivers, *Science of the Total Environment*, 527–539.

Wei, C., Blaschke T., 2018. Pixel-Wise vs. Object-Based Impervious Surface Analysis from Remote Sensing: Correlations with Land Surface Temperature and Population Density, *Urban Science*, 2(1), 1-14.

Wilson, E. H., Hurd, J. D., Civco, D. L., Prisloe, S., Arnold, C., 2003. Development of a Geospatial Model to quantify, Describe and map Urban Growth. *Remote Sensing of Environment*, 86(3), 275–285.

Wong M. S., Nichol J., Lee K., 2010. A Satellite View of Urban Heat Island: Causative Factors and Scenario Analysis, *Korean Journal of Remote Sensing*, 26(6), 617-627.

World Bank Group, 2015. Rising through Cities in Ghana Ghana Urbanization Review Overview Report, International Bank for Reconstruction and Development / The World Bank, Washington DC, USA

World Meteorological Organization, World Health Organization, 2015, Heatwaves and Health: Guidance on Warning-System Development, World Meteorological Organization: Geneva, Switzerland.

Xiaoxiong X., Brian N. W., William L. B., 2009. Overview of NASA Earth Observing Systems Terra and Aqua Moderate Resolution Imaging Spectroradiometer Instrument Calibration Algorithms and On-orbit Performance, *Journal of Applied Remote Sensing*, 3.1-25.

Xu H., Ding F., Wen X., 2009. Urban Expansion and Heat Island Dynamics in the Quanzhou Region, China, *IEEE Journal of Selected Topics in Applied Earth Observations and Remote Sensing*, 2(2), 74-78.

Yu, X., Guo, X. & Wu, Z. 2014. Land Surface Temperature Retrieval from Landsat 8 TIRS—Comparison between Radiative Transfer Equation-Based Method, Split Window Algorithm and Single Channel Method, *Remote Sensing*, 6, 9829-9852.

Non-exclusive licence to reproduce thesis and make thesis public

I, Isaac Kwasi Newton Buo,

1. herewith grant the University of Tartu a free permit (non-exclusive licence) to

reproduce, for the purpose of preservation, including for adding to the DSpace digital archives until the expiry of the term of copyright,

"*Urban Sprawl Dynamics and Urban Heat Islands (UHI) in Ghana*" supervised by Dr. Valentina Sagris and Iuliia Burdun

2. I grant the University of Tartu a permit to make the work specified in p. 1 available to the public via the web environment of the University of Tartu, including via the DSpace digital archives, under the Creative Commons licence CC BY NC ND 3.0, which allows, by giving appropriate credit to the author, to reproduce, distribute the work and communicate it to the public, and prohibits the creation of derivative works and any commercial use of the work until the expiry of the term of copyright.

3. I am aware of the fact that the author retains the rights specified in p. 1 and 2.

4. I certify that granting the non-exclusive licence does not infringe other persons' intellectual property rights or rights arising from the personal data protection legislation.

Isaac Kwasi Newton Buo
Tartu, **27.05.2019**